



Semester Project Report

MSc Nuclear Engineering

# CROCUS Reactor Operation Simulator

**Supervisors:**

Dr. Vincent Lamirand  
Cecilia Montecchio

**Students:**

Caterina Frau  
Matteo Alessandro Meneghini

ZÜRICH - LAUSANNE, SPRING 2025

# Abstract

The project consisted of the development of a real-time simulator of the CROCUS reactor at EPFL. The work was performed by using the already existing simulator of a TRIGA reactor made by JSI as a basis for the code. This was then modified based on the key differences between CROCUS and the JSI TRIGA reactor, and on the purpose of the project. The aim was not to develop an extremely faithful simulator that perfectly reproduced the behaviour of CROCUS, but rather to produce an educational tool that could complement the learning experiences that students have with the CROCUS reactor. Finally, after completing the simulator, a few experiments were conducted on CROCUS and then repeated on the simulator to validate the accuracy of the latter within reasonable limits.

The simulator can be freely downloaded from the [GitHub repository link](#) by following the instructions written in the README file. The code was maintained as open-source, like the JSI code.

# Contents

<b>Abstract</b>	<b>i</b>
<b>Contents</b>	<b>ii</b>
<b>1 Introduction</b>	<b>1</b>
1.1 Project specification . . . . .	1
1.2 CROCUS reactor . . . . .	1
1.3 Base code by JSI . . . . .	2
1.4 CROCUS data . . . . .	4
<b>2 Implementation</b>	<b>6</b>
2.1 Assumptions and simplifications . . . . .	6
2.1.1 Reactivity feedback effects . . . . .	6
2.1.2 Control rods and water level . . . . .	7
2.1.3 Differences between the JSI TRIGA reactor and CROCUS . . . . .	7
2.2 Graphical user interface (GUI) . . . . .	8
2.2.1 Main controls tab . . . . .	9
2.2.2 Control rods tab . . . . .	10
2.2.3 Physics settings tab . . . . .	11
2.2.4 Operational settings tab . . . . .	11
2.2.5 Graph controls tab . . . . .	12
2.2.6 Save data tab . . . . .	13
2.3 Reactivity . . . . .	14
2.3.1 Water level curve . . . . .	15
2.3.2 Control rods curves . . . . .	16
2.4 Displayed graphs . . . . .	16
2.4.1 Doubling time graph . . . . .	17
2.4.2 Count rate graph . . . . .	18
2.5 Operational states . . . . .	19
2.5.1 "Zero" / "Off" state . . . . .	20
2.5.2 "Arret" state . . . . .	20
2.5.3 "Attente" state . . . . .	20
2.5.4 "Inter" state . . . . .	21
2.5.5 "Manuel" state . . . . .	21

<b>3 Experiments and validation</b>	<b>22</b>
3.1 Experimental setup . . . . .	22
3.2 Water level: reactor period measurements . . . . .	23
3.2.1 Experimental method . . . . .	23
3.2.2 Data analysis . . . . .	23
3.2.3 Validation with prior experiments . . . . .	25
3.2.4 Results . . . . .	26
3.2.5 Validation of the simulator . . . . .	27
3.3 Control rods: reactor period measurements . . . . .	30
3.3.1 Experimental method . . . . .	31
3.3.2 Data analysis . . . . .	31
3.3.3 Results and validation . . . . .	31
3.4 Approach to criticality . . . . .	34
3.4.1 Experimental method . . . . .	34
3.4.2 Data analysis . . . . .	34
3.4.3 Validation of the simulator . . . . .	34
<b>4 Discussion and conclusion</b>	<b>36</b>
4.1 Discussion . . . . .	36
4.1.1 Accuracy and performance . . . . .	36
4.1.2 Educational value . . . . .	36
4.1.3 Limitations . . . . .	37
4.1.4 Potential improvements . . . . .	37
4.2 Conclusion . . . . .	38
<b>5 Authors' contributions</b>	<b>39</b>
<b>Bibliography</b>	<b>40</b>
<b>A1 Appendix</b>	<b>41</b>
A1.1 Additional material . . . . .	41

# 1 | Introduction

## 1.1 Project specification

The goal of the project was to develop a functioning real-time operational simulator of the CROCUS reactor. The main purpose was to enable future students to properly understand the physics behind a nuclear reactor and the steps needed to operate CROCUS by providing them with a tool that best simulates the real control board. For this reason, the development of this simulator did not aim to properly recreate the physics of a nuclear reactor, meaning that the simulator is not intended to be used to predict the real behaviour of the reactor in conditions for which it was not developed, i.e. it is not intended for research applications.

## 1.2 CROCUS reactor

CROCUS is a light-water moderated reactor limited, for ease of operation, to a maximum fission power of 100 watts. The reactor has a cylindrical core made up of two distinct concentric fuel zones. The inner fuel zone contains uranium oxide fuel rods enriched to 1.806%, arranged in a square lattice with a pitch of 1.837 cm. The outer fuel zone consists of uranium metal rods with an enrichment of 0.947%, placed in a square lattice with a 2.917 cm pitch. The inner zone includes 336 fuel rods, while the outer zone, since the addition of SAFFRON, comprises 180 rods. The entire core is housed in a tank with a diameter of 132.4 cm, filled with demineralized light water. This water surrounds each fuel rod to ensure effective moderation of fission neutrons, and also provides a sufficient thickness around the outer zone to act as a neutron reflector. The main characteristics of the two types of fuel rods used in CROCUS are detailed in [Table 1.3](#) and [Table 1.4](#). Each rod consists of stacked fuel pellets enclosed in an aluminum cladding, with the space between the fuel and cladding filled with inert helium gas. The rods are held upright by top and bottom grid plates, each of which includes a 0.5 cm layer of cadmium to absorb neutrons leaking axially from the core.

CROCUS has two independent systems for safe shutdown:

- Safety blades: the rapid insertion of two cross-shaped safety rods containing cadmium into the inner fuel region.
- Expansion tanks valves: the rapid opening of four valves causes the water to drain quickly into four separate expansion tanks, leading to a subcritical water level.

Each of these six shutdown mechanisms, the two safety rods and the four drain valves, is capable on its own of bringing the reactor to a safe subcritical state.

Fine power control is achieved either by adjusting the water level in the core or by using two control rods containing  $\text{B}_4\text{C}$  pellets. These control rods are positioned diagonally opposite one another at the edge of the core.

Finally, four neutron detectors, two fission chambers and two  $\text{BF}_3$  counters, are installed at the perimeter of the core, within the water reflector region. These detectors provide essential data on the reactor's condition, including whether it is subcritical (with help from an external neutron source) or critical (monitoring neutron flux, reactor period, and other parameters).

The information reported in this paragraph was retrieved, like the image portraying the top view of the CROCUS reactor ([Figure 1.1](#)), from the document used in the "Radiation and Reactor Experiments" course, at EPFL [[1](#)].

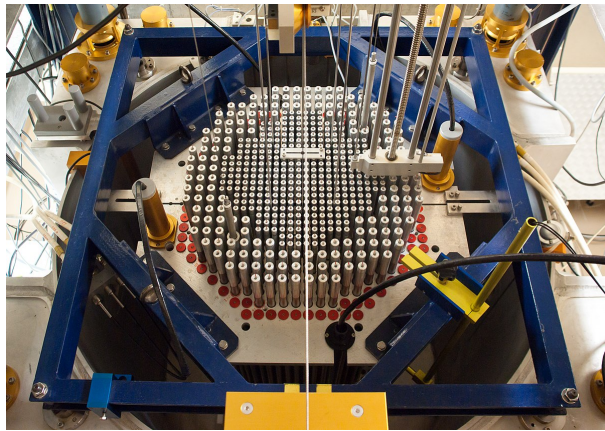


Figure 1.1: Top view of the CROCUS reactor [[1](#)].

### 1.3 Base code by JSI

The development of the simulator started from the solid base provided by the already existing simulator at JSI [[5](#)]. The open-source C++ code was accessed and modified to tailor the simulator to CROCUS, as thoroughly explained later, in [chapter 2](#). The modifications include updating the physical parameters using the data reported in [section 1.4](#), removing superfluous components, incorporating CROCUS-specific elements, and redesigning the graphical user interface (GUI) to better represent the real one.

The JSI code is based on the solution of point kinetics equations ([Equation 1](#), [Equation 2](#)), where the kinetic parameters represent their TRIGA reactor, and the reactivity is given as a function of time, as shown in [Equation 3](#) [[5](#)].

$$\frac{dN(t)}{dt} = \frac{\rho(t) - \beta_{eff}}{\Lambda} N(t) + \sum_{i=1}^6 \lambda_i C_i(t) + S(t) \quad (1)$$

$$\frac{dC_i(t)}{dt} = \frac{\beta_i}{\Lambda} N(t) - \lambda_i C_i(t) \quad i = 1, \dots, 6 \quad (2)$$

$$\rho(t) = \rho_{excess} - \rho_{CR}(t) - \alpha(T(t))T(t) - \rho_{Xe}(t) \quad (3)$$

Where  $N(t)$  is the neutron population,  $\rho(t)$  the reactivity,  $\beta_{eff}$  the total delayed neutrons fraction,  $\Lambda$  the prompt neutron generation time,  $\lambda_i$  the decay constant of the  $i$ -th precursor group,  $C_i(t)$  the concentration of the  $i$ -th precursor group,  $\beta_i$  the delayed neutrons fraction for the  $i$ -th precursor group, and  $S(t)$  the external source of neutrons, which in the updated code is split in two different contributions: the spontaneous fission of uranium, and the external neutron source. The spontaneous fission source is the reason for the non-zero power even when all control rods and safety blades are inserted and the water level is 0 mm. Only six precursor groups are considered because the simulator uses data from the ENDF library.

The time evaluation of the kinetic equations is an iterative process with a fixed time step  $dt = 0.001$  s. The point kinetic equations are solved using an explicit fourth-order Runge-Kutta solver with a fixed step size. From the neutron population  $N(t)$ , the thermal reactor power as well as the integral neutron flux are calculated as in [Equation 4](#) and [Equation 5](#).

$$P(t) = N(t)\Sigma_f v E_f \quad (4)$$

$$\Phi(t) = N(t) \frac{v}{V_c} \quad (5)$$

Where the neutron velocity  $v$  is set to 2200 m/s, considering that the reactor is thermal, the average energy released by fission  $E_f$  is set to 200 MeV,  $\Sigma_f$  is the macroscopic fission cross section, and  $V_c$  is the core volume.

As shown in [Figure 1.2](#), at each time step, the simulator checks whether the reactor is in a pulse and reacts accordingly. Then, the fuel temperature is calculated, the control rods are moved as specified by the user, the Xe and I concentrations are calculated, and the reactivity is recalculated. Then the kinetic equations are propagated, the water temperature is calculated, the operational limits are checked to eventually activate the automatic SCRAM, and finally, the results are pushed to the buffer.

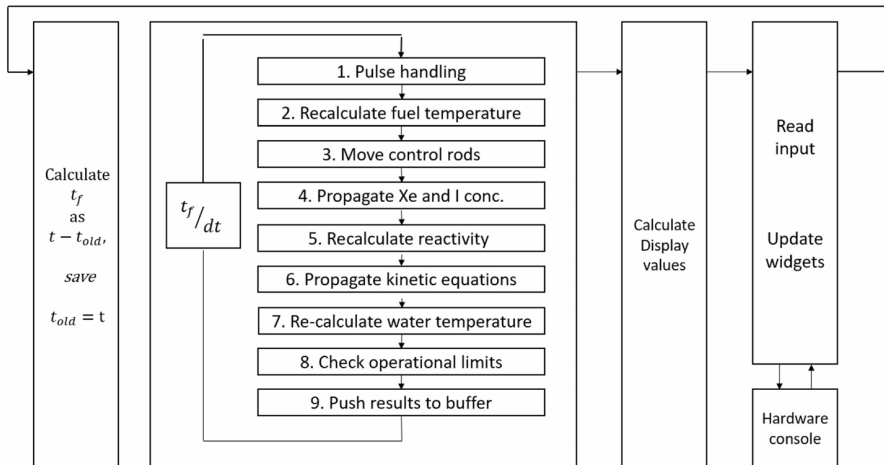


Figure 1.2: Flowchart depicting the operation of the JSI simulator [5].

## 1.4 CROCUS data

All the data reported in this paragraph was retrieved from [6] and [4].

Quantity	Value
$\Lambda$ [s]	$5.9291 \cdot 10^{-5}$
$\beta_1$ [-]	$2.426 \cdot 10^{-4}$
$\beta_2$ [-]	$1.4518 \cdot 10^{-3}$
$\beta_3$ [-]	$1.3533 \cdot 10^{-3}$
$\beta_4$ [-]	$2.9631 \cdot 10^{-3}$
$\beta_5$ [-]	$1.1026 \cdot 10^{-3}$
$\beta_6$ [-]	$3.468 \cdot 10^{-4}$
$\lambda_1$ [s <sup>-1</sup> ]	$1.291 \cdot 10^{-2}$
$\lambda_2$ [s <sup>-1</sup> ]	$3.138 \cdot 10^{-2}$
$\lambda_3$ [s <sup>-1</sup> ]	$1.187 \cdot 10^{-1}$
$\lambda_4$ [s <sup>-1</sup> ]	$3.163 \cdot 10^{-1}$
$\lambda_5$ [s <sup>-1</sup> ]	$1.197 \cdot 10^0$
$\lambda_6$ [s <sup>-1</sup> ]	$3.495 \cdot 10^0$

Table 1.1: Kinetic parameters of CROCUS.

Quantity	Value
$D_{core}$ [m]	0.6
$H_{core}$ [m]	1
$D_{vessel}$ [m]	1.3

Table 1.2: Size quantities of CROCUS.

The core volume, which is needed for the calculation of the flux (Equation 5), can be calculated from the quantities shown in Table 1.2.

$$V_{core} = H_{core} \frac{D_{core}^2 \pi}{4} = 0.283 \quad [m^3] \quad (6)$$

As explained in section 1.2, there are two different concentric fuel zones in the reactor. The quantities of the inner zone ( $UO_2$ ) are shown in Table 1.3, while those of the outer zone (metallic U) in Table 1.4.

Quantity	Value
Number of rods [-]	336
Fuel density [g·cm <sup>-3</sup> ]	10.56
Enrichment [%]	1.81
Rod diameter [cm]	1.05
Rod height [cm]	100

Table 1.3: Specifics of the inner fuel zone.

Quantity	Value
Number of rods [-]	180
Fuel density [g·cm <sup>-3</sup> ]	18.68
Enrichment [%]	1
Rod diameter [cm]	1.7
Rod height [cm]	100

Table 1.4: Specifics of the outer fuel zone.

From these two tables, one can compute the intensity of the spontaneous fission source to be implemented in the simulator as follows: for each fuel zone calculate their total volume, then

the total mass of fuel, then the total number of atoms of  $^{238}\text{U}$  and of  $^{235}\text{U}$ , then the total number of atoms of the two isotopes by summing the quantities relative to the two fuel zones, then the neutron source intensity for each isotope by considering their half-lives, spontaneous fission branching ratio, and average number of neutron emitted by spontaneous fission. Finally, the total spontaneous fission source is the sum of the contributions of the two isotopes.

$$V_{tot,i} = N_{rods,i} \cdot H_i \frac{D_i^2 \pi}{4} \quad (7)$$

$$m_{tot,i} = V_{tot,i} \cdot \rho_i \quad (8)$$

$$N_{U8,1} = \frac{m_{tot,1} \cdot N_A}{238} \cdot (1 - \epsilon_1) \cdot \frac{(1 - \epsilon_1) \cdot 238 + \epsilon_1 \cdot 235}{(1 - \epsilon_1) \cdot 238 + \epsilon_1 \cdot 235 + 2 \cdot 16} \quad (9)$$

$$N_{U5,1} = \frac{m_{tot,1} \cdot N_A}{235} \cdot \epsilon_1 \cdot \frac{(1 - \epsilon_1) \cdot 238 + \epsilon_1 \cdot 235}{(1 - \epsilon_1) \cdot 238 + \epsilon_1 \cdot 235 + 2 \cdot 16} \quad (10)$$

$$N_{U8,2} = \frac{m_{tot,2} \cdot N_A}{238} \cdot (1 - \epsilon_2) \quad (11)$$

$$N_{U5,2} = \frac{m_{tot,2} \cdot N_A}{235} \cdot \epsilon_2 \quad (12)$$

$$N_{Uj} = N_{Uj,1} + N_{Uj,2} \quad (13)$$

$$SF_{U8} = \bar{\nu}_{sf,U8} \cdot N_{U8} \cdot \frac{\ln(2)}{T_{1/2,U8}} \cdot BR_{sf,U8} \quad (14)$$

$$SF_{U5} = \bar{\nu}_{sf,U5} \cdot N_{U5} \cdot \frac{\ln(2)}{T_{1/2,U5}} \cdot BR_{sf,U5} \quad (15)$$

The resulting value of the spontaneous fission source is shown in [Table 1.5](#).

Quantity	Value
SF <sub>U8</sub> [ $\#\cdot\text{s}^{-1}$ ]	$1.435 \cdot 10^4$
SF <sub>U5</sub> [ $\#\cdot\text{s}^{-1}$ ]	$1.263 \cdot 10^{-1}$
External source [ $\#\cdot\text{s}^{-1}$ ]	$10^7$

Table 1.5: Neutron sources in CROCUS.

# 2 | Implementation

## 2.1 Assumptions and simplifications

To develop the simulator, all the assumptions made by the developers at JSI for their simulator were used. The characteristics of CROCUS and its differences from the JSI TRIGA reactor allowed for further simplifications, which are discussed in this section.

### 2.1.1 Reactivity feedback effects

Since CROCUS is a zero-power reactor operated at temperatures between 17.5°C and 22.5°C, the thermal feedback effects are negligible in the computation of the total reactivity. For the same reason, the same can be said about the reactivity effect of Xe, and is demonstrated as follows: neglecting the decay from  $^{135}\text{Te}$  to  $^{135}\text{I}$  ( $\beta$ - decay with a 19 s half-life) and the destruction of  $^{135}\text{I}$  by neutron capture, the Bateman equations for  $^{135}\text{I}$  and  $^{135}\text{Xe}$  become:

$$\frac{dN_I}{dt} = \gamma_I N_{U5} \sigma_{U5}^f \Phi - \lambda_I N_I \quad (16)$$

$$\frac{dN_{Xe}}{dt} = \gamma_{Xe} N_{U5} \sigma_{U5}^f \Phi + \lambda_I N_I - \lambda_{Xe} N_{Xe} - N_{Xe} \sigma_{Xe}^c \Phi \quad (17)$$

At steady state, the  $^{135}\text{Xe}$  concentration becomes:

$$N_{Xe} = \frac{\lambda_I N_I + \gamma_{Xe} N_{U5} \sigma_{U5}^f \Phi}{\lambda_{Xe} + \sigma_{Xe}^c \Phi} = N_{U5} \frac{(\gamma_I + \gamma_{Xe}) \frac{\sigma_{U5}^f}{\sigma_{Xe}^c \Phi}}{1 + \frac{\lambda_{Xe}}{\sigma_{Xe}^c \Phi}} \quad (18)$$

Assuming an infinite reactor (no leakage), the reactivity change due to the formation of  $^{135}\text{Xe}$  is given by:

$$\Delta\rho_{Xe} = \frac{k - k_0}{k} = \frac{\eta\epsilon p f - \eta\epsilon p f_0}{\eta\epsilon p f} = \frac{f - f_0}{f} = \frac{\frac{\Sigma_a^F}{\Sigma_a^F + \Sigma_a^m + \Sigma_a^{Xe}} - \frac{\Sigma_a^F}{\Sigma_a^F + \Sigma_a^m}}{\frac{\Sigma_a^F}{\Sigma_a^F + \Sigma_a^m + \Sigma_a^{Xe}}} = -\frac{\Sigma_a^{Xe}}{\Sigma_a^F + \Sigma_a^m} \quad (19)$$

$k_0$  can also be written as:

$$k_0 = 1 = \eta\epsilon p f_0 = \frac{\nu\Sigma_f}{\Sigma_a^F} \epsilon p \frac{\Sigma_a^F}{\Sigma_a^F + \Sigma_a^m} \quad (20)$$

$$\Sigma_a^F + \Sigma_a^m = \nu\Sigma_f \epsilon p \quad (21)$$

Where  $\Sigma_f = N_{U5}\sigma_{U5}^f$ . Then the reactivity change can be written as:

$$\Delta\rho_{Xe} = -\frac{N_{Xe}\sigma_{Xe}^c}{\nu N_{U5}\sigma_{U5}^f \epsilon p} = -\frac{\gamma_I + \gamma_{Xe}}{\nu \epsilon p \left(1 + \frac{\lambda_{Xe}}{\sigma_{Xe}^c \Phi}\right)} \quad (22)$$

Therefore, since the integral flux in CROCUS is always smaller or equal to  $2.5 \cdot 10^9 \text{ cm}^{-2}\text{s}^{-1}$  [4], the reactivity effect of Xe is always negligible.

Since no feedback effects are considered in the simulator, there is no distinction between actual and inserted reactivity. In the JSI simulator, this difference was displayed to highlight the feedback effects, while in the CROCUS simulator, only the inserted reactivity is displayed.

### 2.1.2 Control rods and water level

The control rods, as well as the water level, were modelled assuming no inertia, meaning that they always move at a constant speed, with infinite acceleration between stationary and moving states and vice versa. Furthermore, for the water level, no fluid inertia was taken into account, hence the water level was assumed to coincide with the position of the spillway precisely. Regarding their reactivity worth curves, no interdependency was taken into account; for instance, the reactivity contribution from a control rod insertion was considered independent of the water level. This is clearly wrong, as inserting a control rod by any amount with the water level at 990 mm rather than 940 mm does not result in the same reactivity insertion; however, this is how it was implemented for simplicity. The validity of this assumption is further discussed in [subsection 3.3.3](#).

### 2.1.3 Differences between the JSI TRIGA reactor and CROCUS

The differences between the JSI TRIGA reactor and CROCUS led to several major changes for the development of the simulator:

- The neutron source in CROCUS is constant and its intensity cannot be represented by other types, unlike in the JSI TRIGA reactor, where the source type can be moved in and out automatically, and its intensity can thus be constant, square wave, sine wave, or saw tooth.
- The operation mode in CROCUS is exclusively manual, unlike in the JSI TRIGA reactor, where the control rods can be moved automatically based on the operation mode, which can be square wave, sine wave, saw tooth, or automatic.
- The automatic SCRAM signals in CROCUS are related exclusively to doubling time, reactor power, and power from the grid. In the JSI TRIGA reactor, they also comprise the fuel temperature and water temperature. These two SCRAM signals were removed, and the SCRAM caused by the loss of grid power was not implemented.
- The TRIGA reactor can operate in pulses, while CROCUS cannot; therefore, the pulse mode was removed from the simulator.

Other differences between the JSI TRIGA reactor and the CROCUS reactor are about fuel composition and size. In the simulator, all of these quantities had to be changed. The data relative to CROCUS is reported in [section 1.4](#).

Considering all of these assumptions and simplifications, the flowchart of the operation of the simulator is different than the one shown in [Figure 1.2](#): pulse handling, fuel temperature calculation, Xe and I concentrations calculation, and water temperature calculation are removed, and the movement of the water level is added. Moreover, the check of the operational limits consists of checking only the values of the doubling time and power. All other steps remained unchanged.

## 2.2 Graphical user interface (GUI)

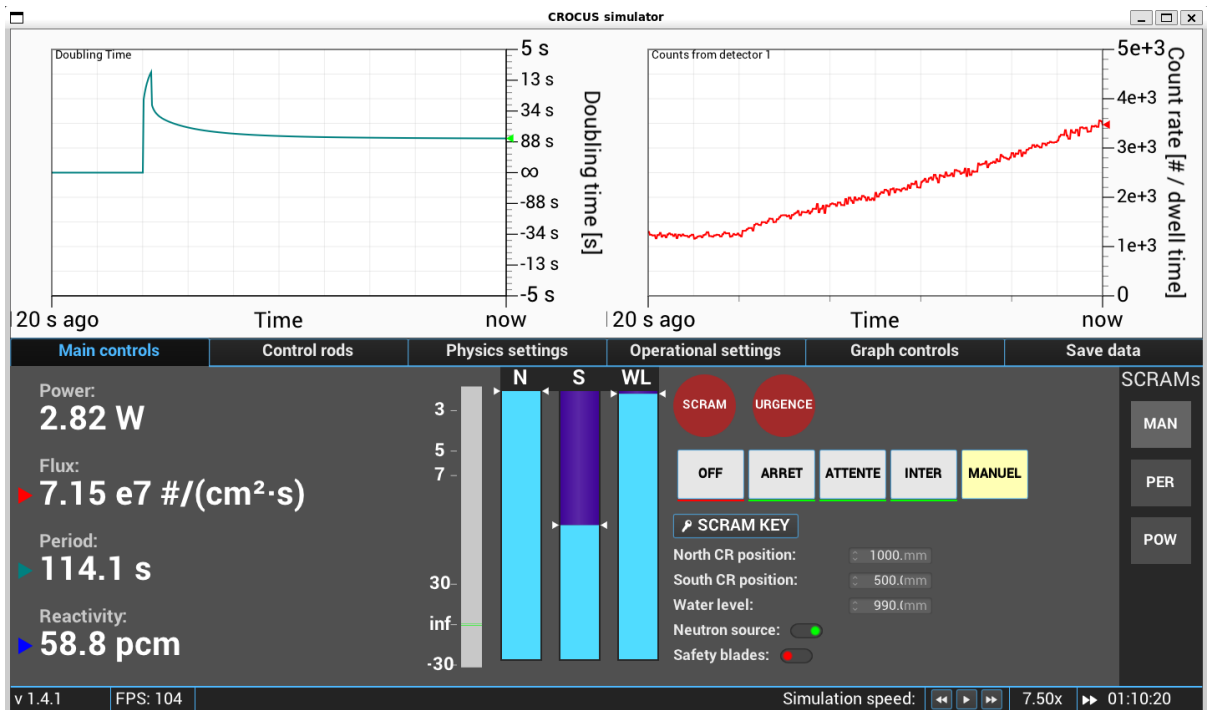


Figure 2.1: Screenshot of the simulator GUI.

[Figure 2.1](#) shows how the simulator presents itself to the user. The GUI is structured to best represent how the information is displayed in the real control room of CROCUS, with graphs displaying the doubling time and count rate in real time in the upper half, and tabs with all other types of information in the bottom half. The upper edge contains buttons for the scaling of the software window on the user's computer, while with the buttons in the bottom edge, the user can choose the speed of the simulation. This section is dedicated to explaining the information that the tabs contain, while [section 2.4](#) explores how the displayed graphs were implemented.

## 2.2.1 Main controls tab

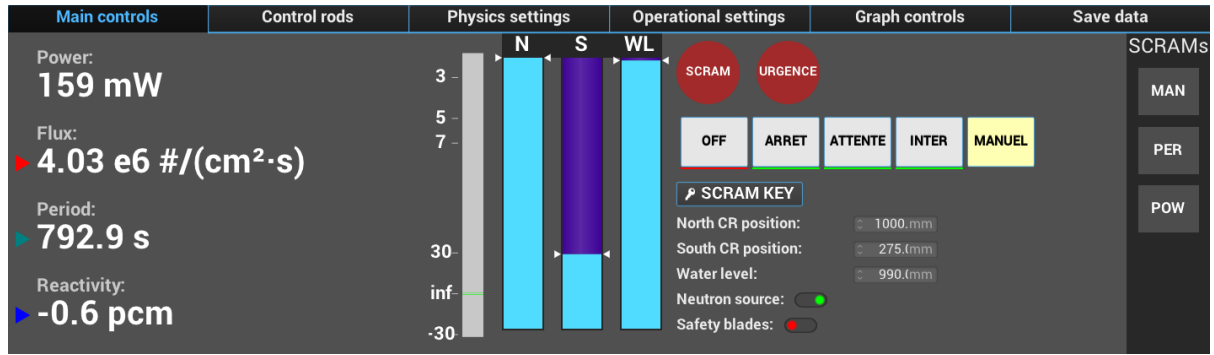


Figure 2.2: Screenshot of the main controls tab.

The main controls tab is the default tab once the simulator is started, and it is also the most important one, since it simulates, in a simplified version, the control board of CROCUS.

On the left, the main quantities that describe the reactor physics are displayed: power, flux, period, and reactivity. The ways these values are obtained are explained in different sections of this report. Although the main graph displays the doubling time, the choice was to show the period in the main controls tab since that is the more important quantity from a reactor physics perspective.

The grey bar in the middle shows in green the value of the period. The three blue bars beside it show the position of the control rods and water level. Above them, "N", "S", and "WL" refer to the North control rod, the South control rod, and the water level, respectively.

On the right are the controls that the user can interact with. As on the real control board, two red buttons allow at all times to manually SCRAM the reactor or shut it down because of an emergency. Below those two buttons are the buttons relative to the operational states of CROCUS, further explained in [section 2.5](#). Further down is the "SCRAM key" button, which was implemented to simulate the need for a key after the reactor is manually SCRAMmed. Then there are interactive boxes, in which the user can insert the position to which they want the control rods and the water level to go, with a precision of 0.1 mm. As reported in [Table 2.3](#), these are accessible only in the "Manuel" state. Finally, two widgets show the positions of the neutron source and safety blades. The neutron source widget is clickable to manually insert or remove the source (only in the "Inter" and "Manuel" states, [Table 2.3](#)), while the safety blades cannot be operated by the user. They are instead automatically inserted or withdrawn depending on the operational state of the reactor, the widget serving only to show their position.

The rightmost column contains the SCRAM signals. In case of a SCRAM, the signal that activated it is highlighted in red. "MAN" stands for manual, i.e. the user pressed the "SCRAM" button, "PER" stands for period, and "POW" stands for power. Furthermore, for any type of shutdown, the corresponding message is shown in the bash from which the simulator was opened.

## 2.2.2 Control rods tab

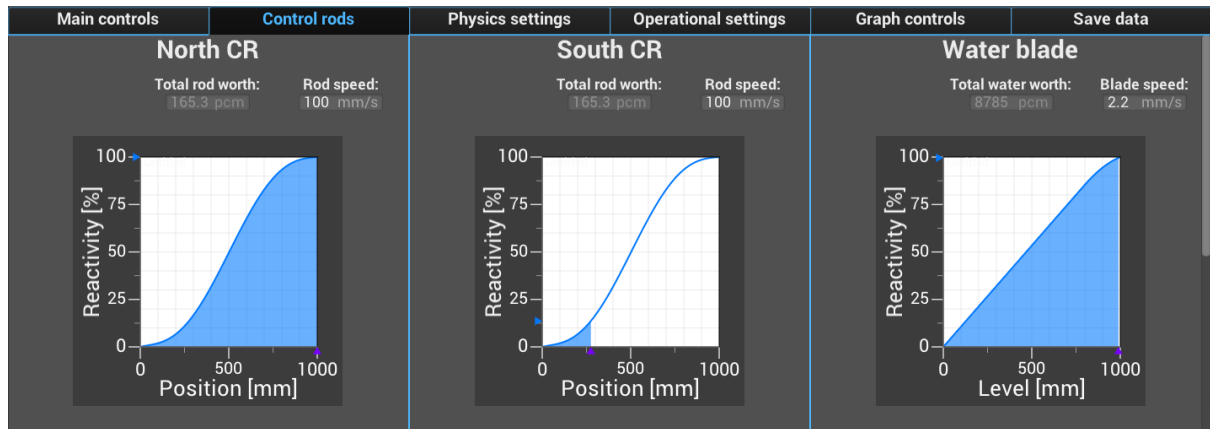


Figure 2.3: Screenshot of the control rods tab (upper part).

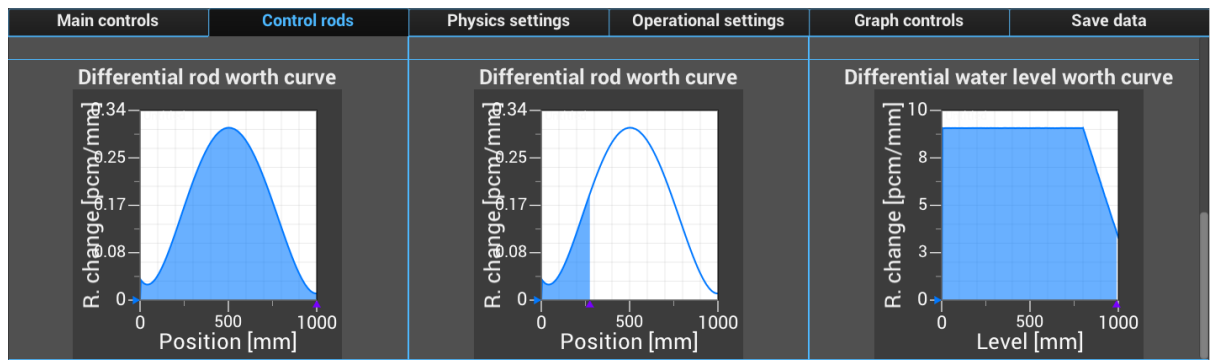


Figure 2.4: Screenshot of the control rods tab (lower part).

The control rods tab contains all information regarding the reactivity worths and speed of the control rods and water level. There is one column for each of these three elements.

As shown in [Figure 2.3](#), in the upper part of the tab, the user can modify the total worths of the control rods and water, as well as their speed (for the water level, the speed of the spillway in the range 800 - 1000 mm). Below these boxes, there are the reactivity curves of the three elements, further discussed in [section 2.3](#). The curves are filled in real time as the elements move in the core; the graphs presented in this figure correspond to the same configuration of [Figure 2.2](#).

In [Figure 2.4](#), the graphs display the derivatives of the reactivity curves; therefore, the coloured areas correspond to the total reactivity inserted for each element. These graphs, even more than the previous ones, help the user visualize that a given displacement of a control rod has different effects depending on its initial and final positions.

Since the reactivity worth curve of the water that was implemented is quadratic in the range between 800 mm and 1000 mm (see [subsection 2.3.1](#)), its derivative is linear. This is a valid approximation, given the curve provided in the safety report [4], reported in [Figure A1.2](#). Especially around the critical water level, which is the region of interest, the derivative curve can be approximated to a linear curve with values that coincide with the ones of the derivative

of the implemented curve ( $\sim 4.15$  pcm/mm).

### 2.2.3 Physics settings tab

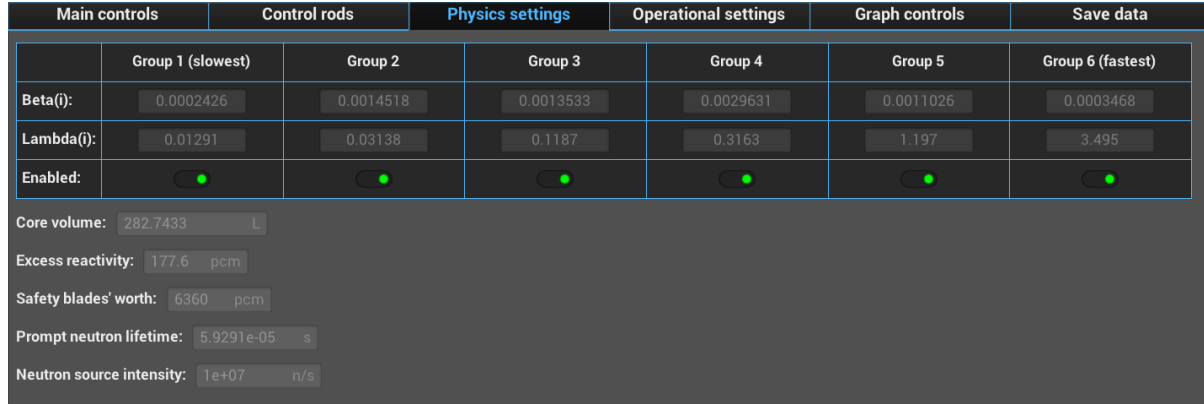


Figure 2.5: Screenshot of the physics settings tab.

In the physics settings tab, the user can tweak the configurational parameters of CROCUS. They can modify the  $\beta$  and  $\lambda$  values of the six precursors' groups and even disable them. They can also modify the values of the core volume, which influences the flux, of the excess reactivity, which influences the critical water level, of the safety blades' worth, of the prompt neutron lifetime, and of the neutron source intensity.

### 2.2.4 Operational settings tab

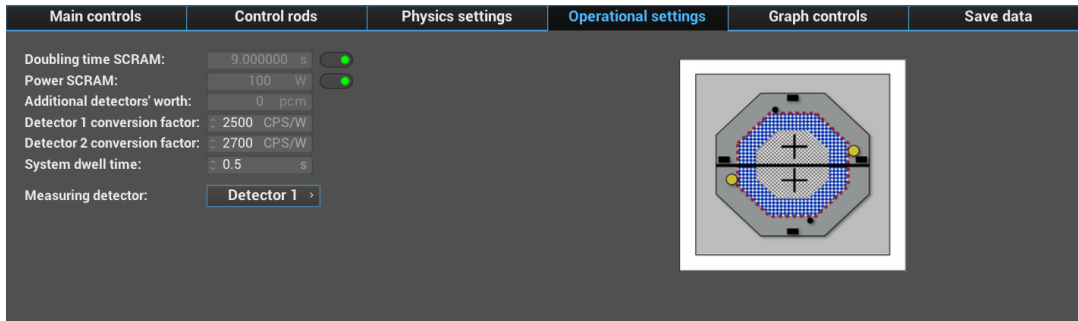


Figure 2.6: Screenshot of the operational settings tab.

This tab includes settings related to the operational limits and the variables related to the use of the simulated detectors, connected to the neutron data displayed and saved. The thresholds for the automatic SCRAM were found in the safety report of the reactor [4]. These can be modified and turned off by the user, before the simulation is started (Table 2.3).

The other settings present in the tab are related to the simulated detectors measuring the neutron counts, described in section 1.2. The counts measured in the control room come from two different fission chambers positioned in the proximity of the core in the reflector region, and the reactor operator can decide which data to view on the screen (from which detector). Detectors can be positioned with different orientations and therefore capture more or fewer

neutrons at a given power; for this reason, a conversion factor was introduced in the simulator to obtain the counts per second of the measurement based on the selected detector.

Given the extensive ongoing research in CROCUS, a range of detectors are continuously being added or removed to perform a variety of experiments. To allow the user to simulate all these different types of configurations, an interactive box was added to account for the negative reactivity worth of additional detectors placed in the reactor. The value inserted in that box is automatically removed from the excess reactivity.

Included in this tab is also the dwell time setting, i.e., the integration time of the measured counts, which, for the real reactor, is adjusted within the detectors data visualization software GENIE-2000, based on considerations regarding the accuracy to be obtained from the data and the total time of the experiment. This is a quantity that students should familiarize themselves with to carry out CROCUS-related experiments most effectively, and for this reason it was incorporated into the simulator. This variable affects the display of the count rate, explained in [subsection 2.4.2](#), and the output file that can be downloaded, described in more detail in [subsection 2.2.6](#).

Lastly, the user can choose which detector measurement to display on the plotting screen, as explained in more detail in [section 2.4](#).

A special mention should be made for the inclusion of the CROCUS design specification image on the right, as featured in the real control room.

## 2.2.5 Graph controls tab

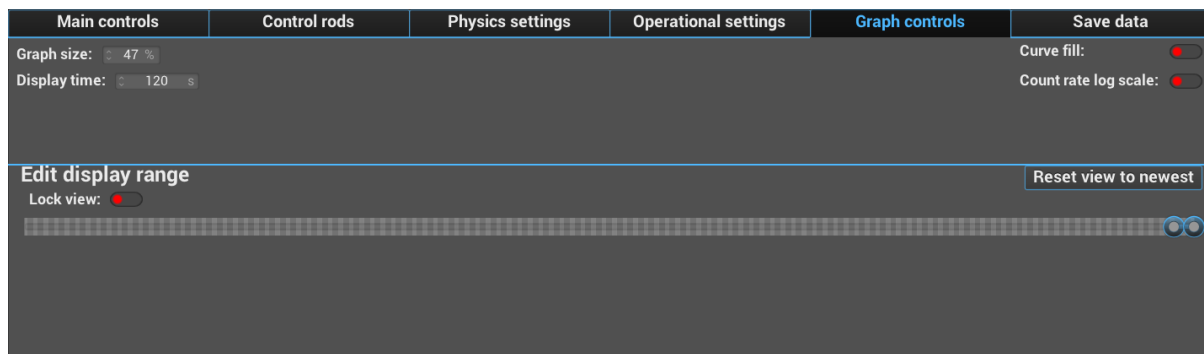


Figure 2.7: Screenshot of the graph controls tab.

The graph controls tab contains the tools relative to the graphs displayed in the upper half of the simulator GUI. The user can choose to have larger graphs and smaller tabs or vice versa. The graphs automatically display the trends of the last 120 seconds, but this time interval is also modifiable. On the right side, the user can choose to fill the curves and also to apply a log scale to the y-axis of the count rate graph. In the bottom part of the tab, the user can choose to display any time interval they want since the start of the simulation.

## 2.2.6 Save data tab

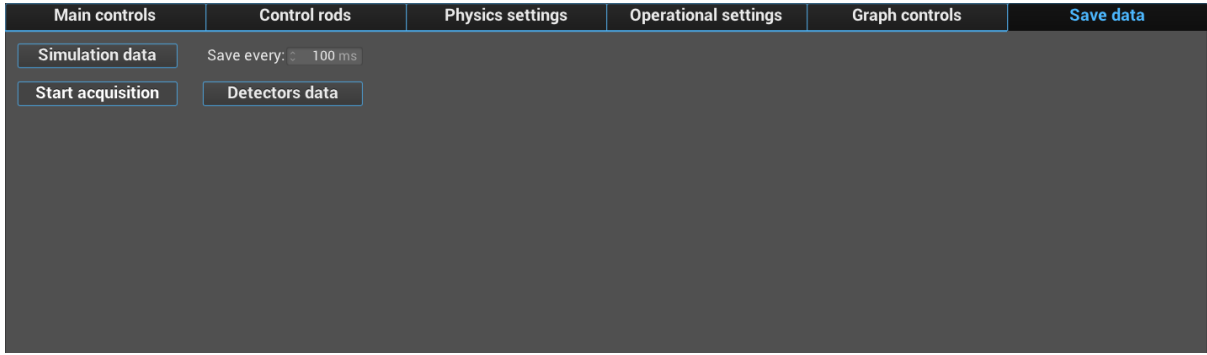


Figure 2.8: Screenshot of the save data tab.

The save data tab, presented in [Figure 2.8](#), is dedicated to the collection of selected variables so that a log of the performed simulation is stored in a .dat file. A first button, *Simulation data*, allows up to 3h of recording of the simulation time, automatically saved until the last time frame once the button is pressed. The user can choose the frequency of the printout of variables. The displayed quantities were chosen to enable the simulation steps to be reconstructed as effectively as possible. A snippet of a log is shown in figure [Figure 2.9](#): together with presenting the values of reactivity, power, neutron flux and reactor period, the positions of the control rods, water level, safety blades and neutron source are printed.

```
#####
# Research reactor simulator log Tue Jun 17 23:11:35 2025 #
#Time[h:m:s:ms] n-source Safety blades NR[mm] SR[mm] WL[mm] Reactivity[pcm] Power[W] Flux[#/cm²·s] Period[s]
#####
02:43:37:126 OUT OUT 1000 280 995 18.514 0.20698 5.2367e+06 431.87
02:43:38:126 OUT OUT 1000 280 995 18.514 0.20746 5.2489e+06 431.93
02:43:39:126 OUT OUT 1000 280 995 18.514 0.20795 5.261e+06 431.99
02:43:40:126 OUT OUT 1000 280 995 18.514 0.20843 5.2732e+06 432.05
02:43:41:126 OUT OUT 1000 280 995 18.514 0.20891 5.2854e+06 432.11
02:43:42:126 OUT OUT 1000 280 995 18.514 0.20939 5.2977e+06 432.17
02:43:43:126 OUT OUT 1000 280 995 18.514 0.20988 5.3099e+06 432.22
```

Figure 2.9: Example of output printed with the *Simulation data* button.

In addition, a method for collecting data generated by the simulated detectors was implemented, as described in more detail in [subsection 2.4.2](#), which discusses the graph where the number of neutron counts is plotted. By pressing the *Start acquisition* button, the simulator starts writing data to an output file, a screenshot of which is shown in [Figure 2.10](#). Here, the counts from both detectors are printed together with the simulation time to keep track of the evolution. The first button remains highlighted until the *Detectors data* button is pressed, which stops data recording and allows the saving of the file. As this second acquisition is specifically related to the detectors, the integration time selected for the measurement (dwell time) is indicated at the top of the output file, and cannot be modified from the *Operational setting* tab during the recording.

This addition was specifically designed to have a simulated equivalent of the CROCUS experimental measurements file, hence the key difference in the start-stop capture feature in com-

##### Counts/bin from detectors, dwell Time = 0.04 s #####		
Time[h:m:s:ms]	Det1[Counts]	Det2[Counts]
04:07:00:625	74	58
04:07:00:665	71	53
04:07:00:705	66	68
04:07:00:745	47	51
04:07:00:785	52	77
04:07:00:825	54	55
04:07:00:865	43	73
04:07:00:905	46	83
04:07:00:945	70	56

Figure 2.10: Screenshot of an example of output printed with the *Detectors data* button.

parison to the total output file (*Simulation data* button), which collects all history information with no option to start from a specific instant.

## 2.3 Reactivity

As explained in [section 2.1](#), the definition of the reactivity used to solve the point kinetics was drastically modified: the thermal and Xe feedback effects were removed, and the contribution of the water level was added. The reactivity at any instant is then defined as:

$$\begin{aligned} \rho(t) = & \rho_{\text{excess}} - \rho_{\text{SB}}(t) + \\ & + (\rho_{\text{CR, North}}(t) + \rho_{\text{CR, South}}(t) + \rho_{\text{WL}}(t)) + \\ & - (\rho_{\text{CR, North, tot}} + \rho_{\text{CR, South, tot}} + \rho_{\text{WL, tot}}) \end{aligned} \quad (23)$$

Where *SB* stands for "safety blades", *CR* for "control rod", and *WL* for "water level". At each step of the evaluation of the kinetic equations, the reactivity worth of each control rod, as well as that of the water level, is computed based on their position and their reactivity curve. Because of how the total reactivity is defined, the CR and WL curves are positive at all points, equal to their total worth at the top position, where the WL is 1000 mm and the CRs are fully withdrawn, and equal to 0 at the bottom position, where the WL is 0 mm and the CRs are fully inserted. The reactivity is thus computed by removing the total worths of CRs and WL, and then adding the reactivity worth based on their position.

The safety blades were modelled to be either completely inserted or withdrawn from the core, and their insertion and removal were approximated to be instantaneous. Moreover, the two safety blades cannot be inserted and withdrawn during operation nor operated individually; instead, as explained in [section 2.5](#), they are both automatically withdrawn when the reactor is in the "Manuel" state, and automatically inserted during shutdown or SCRAM. Each safety blade is worth 3180 pcm [4].

The curves of reactivity worths of the control rods and water level are discussed in the next two paragraphs.

### 2.3.1 Water level curve

The reactivity worth curve for the water level was obtained empirically as explained in section 3.2. The measurements were conducted at water levels of 925, 935, 965, 975, and 985 mm ( $\pm 0.1$  mm for each), and the critical water level was known to be at  $(956.2 \pm 0.1)$  mm. Utilizing the results from these experiments (Table 3.3), a quadratic curve was fitted and later implemented in the simulator for all water levels between 800 and 1000 mm. For water levels below 800 mm, the curve was assumed linear and with the same slope as the derivative of the fitted curve at 800 mm. The latter assumption was made purely for simplicity and with no theoretical base, simply because water levels below 800 mm are of no interest for the operation of the reactor (the water level cannot be lowered below 800 mm in the "Manuel" state, subsection 2.5.5). The choice to fit a quadratic curve for water levels between 800 and 1000 mm was taken based on the shape of the curve given in the safety report [4], reported in Figure A1.1.

The results from the measurement at 925 mm were excluded from the fit because they skewed the curve to reactivity values which are in disagreement with those documented in the safety report. This choice was made also because the measurement was deemed inaccurate, given that the threshold to compute the adjustment time had to be raised to 5%, as discussed in subsection 3.2.2. The curve was obtained by performing a fit with the following shape:

$$\rho(WL) = A \cdot WL^2 + B \cdot WL + C \quad (24)$$

Where  $\rho$  is in pcm and  $WL$  in mm. The confidence interval was obtained by performing the fit 10000 times with a Monte Carlo method, where both water level and reactivity were assumed to follow normal distributions with the standard deviations given in Table 3.3. The fit curve and the  $1\sigma$  confidence interval are shown in Figure 2.11, while the parameters of the fit are reported in Table 2.1.

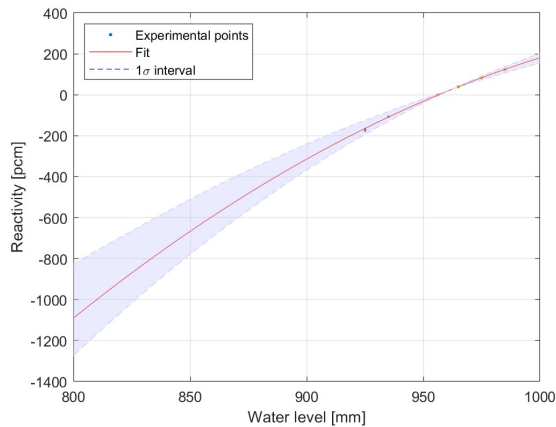


Figure 2.11: Reactivity worth of the water level.

As can be noted from Equation 23, since the experiment was conducted with both control rods withdrawn (i.e.  $\rho_{CR} = 0$ ), the value of the fitted curve at  $WL = 1000$  mm corresponds to the excess reactivity, reported in Table 2.2.

Parameter	Value from the fit	Value implemented in the simulator
A [pcm/mm <sup>2</sup> ]	-0.0150 ± 0.006	-0.014996
B [pcm/mm]	33 ± 11	33.392
C [pcm]	-18000 ± 5000	-18395

Table 2.1: Parameters of the fit  $\rho = A \cdot WL^2 + B \cdot WL + C$ .

	Value from the fit	Value implemented in the simulator
$\rho_{excess}$ [pcm]	178 ± 18	177.63

Table 2.2: Excess reactivity in CROCUS extrapolated from experimental results.

As explained in the previous paragraph, the way the total reactivity is defined ([Equation 23](#)) requires a WL curve that is fully positive. To obtain such a curve, the parameter C was reduced by a value equal to  $\rho_{excess}$ , and then the whole curve was shifted upwards by the total water worth, which is simply the difference between the value of reactivity at WL = 1000 mm and that at WL = 0 mm. The parameters reported in [Table 2.1](#) already correspond to the curve before the upward shift. [Figure 2.11](#) presents the curve with both negative and positive values to show the fit of the experimental points, which are also plotted with their uncertainty bars (not noticeable).

### 2.3.2 Control rods curves

The two rods, North and South, were considered to have the same total reactivity worth and the same reactivity curve, as past experiments have already proved. The curve was retrieved from the "Control rod calibration" document [3], and is reported in [Equation 25](#).

$$\begin{aligned} \rho(CR) = & -192.39 \cdot CR^6 + 1690.9 \cdot CR^5 - 3473.6 \cdot CR^4 \\ & + 2363.3 \cdot CR^3 - 260.91 \cdot CR^2 + 37.974 \cdot CR \end{aligned} \quad (25)$$

Where  $\rho$  is in pcm while  $CR$  in m. As required by [Equation 23](#), the curve is fully positive and equal to the total rod worth for  $CR = 1$  m (1000 mm), and to 0 for  $CR = 0$  mm.

This curve corresponds to a configuration where the water level is at 1000 mm. As explained in [section 2.1](#), the reactivity curves of the control rods were modelled as independent of the water level. The validity of this assumption is discussed in [subsection 3.3.3](#).

## 2.4 Displayed graphs

In order to replicate the real CROCUS control room operations as closely as possible, the main graphs tab has been completely renovated from the JSI version. As can be seen from [Figure 2.12](#), this section of the GUI is now split into two graphs showing the evolution in time of the doubling time and the count rate from the selected detector.

The choice stems from the fact that, when working in the control room, these are the two possible quantities to monitor and of most interest to students.

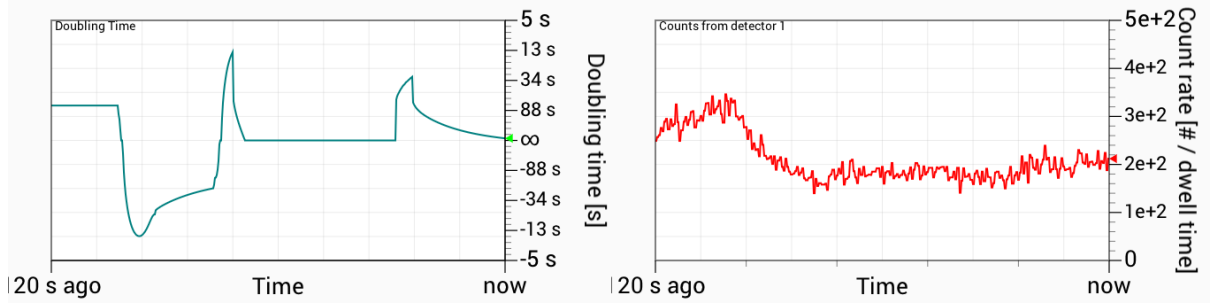


Figure 2.12: Screenshot of the upper half of the simulator GUI.

### 2.4.1 Doubling time graph

Doubling time (DT) is defined as the interval required for a reactor's neutron population (and therefore its power) to increase or decrease (negative sign) by a factor of two. Because it directly reflects the speed of the chain reaction's growth or decay, it serves as an immediate indicator of how fast the power is changing inside the core. It is constantly monitored in the real control room through one of the screens, and therefore it was decided to include it in the simulator. The doubling time is obtained from the reactor period using [Equation 26](#), which is in turn calculated at each time step with the means of an exponentially weighted moving average defined in [Equation 27](#).

$$DT = \tau \cdot \ln(2). \quad (26)$$

$$\tau_{reactor} = \Delta t \cdot \frac{\sum_{i=0}^{N-2} \frac{k^{N-i-2}}{\ln(r_i)}}{\frac{1 - k^{N-1}}{1 - k}} \quad (27)$$

Where:

- $\Delta t$ : time step between two consecutive power measurements.
- $r_i = \frac{P_{i+1}}{P_i}$ : power ratio between consecutive steps.
- $k = 0.01$ : exponential weighting factor (i.e., older data is exponentially down-weighted).
- $N$ : number of steps included in the moving average.

As shown in [Figure 2.12](#), the axis scale is not the conventional upward-growing, which could fail at capturing the most critical region of low DT and at the same time lose information at large periods, when the reactor is in a stable condition. The used scale inverts this emphasis: the DT values are “folded” around the centre, meaning that very short periods (following rapid power excursions) are pushed to the outer edges, whereas increasingly long periods collapse toward the middle, with the exact centre marking infinite period. In this way, it is also easily possible to follow negative reactivity insertions that lead to a negative period, and therefore doubling time, resulting, for instance, from a water level reduction or a control rod insertion.

This rescaling of the graph was obtained by first squeezing the calculated doubling time into a 0-1 band with logarithmic importance. This was then flipped, so short DT come out near 1 and long ones near 0, and assigned the right sign, pushing positive periods upward and negative ones downward. The exact opposite mathematical steps were used to build the axis, turning those compact numbers back into the real doubling time seconds, and assigning the infinity symbol to the mid-value (0), depicting stable periods. In this way, the curve is computationally easy to plot, and the labels are made familiar to read for the user.

#### 2.4.2 Count rate graph

This plot was meant to be as similar as possible to the output coming from the detectors' visualization software, where the neutron detections are displayed as number of counts over time bins. The time bins are as large as the dwell time, hence the axis label.

In real operations, these neutron counts are subjected to Poissonian statistical fluctuations clearly visible from the display. On the other hand, the simulator calculation would deliver a perfectly smooth count rate, hence the need to implement the physical noise, also for validation purposes. This is achieved in the code as follows:

- The physics model of the programme calculates the ideal count rate at every millisecond (time step of the simulation).
- This is integrated over a user-defined running total, the dwell time, and the final sum of the number of counts per time bin is stored in a vector.
- The randomness in this value to reflect real fluctuations is then added as follows:
  - If the total value is small, the code samples a value from a Poisson distribution with  $\lambda$  equal to the value.
  - If instead it is large enough ( $\lambda > 100$  counts per dwell time), it uses a normal Gaussian distribution with mean equal to variance, an approximation that allows for a faster computation and is accurate at high counts.
- The random result, rounded to an integer, is then held constant and reported for every millisecond throughout the next dwell period, before the whole cycle is repeated.

By plotting the resulting vector, it is finally possible to follow the evolution in time of the count rate as "measured" from the simulated detectors with introduced noise; evolution that also takes into account the integration time set in the *Operational settings* tab. This means that if the dwell time is doubled, the number of neutrons counted will accordingly increase of a factor of 2 in the plot.

This entire process was also useful for a comparison with the real reactor data for the validation of the simulator: the results are always saved in a defined dwell time; therefore, it was possible to apply the same procedures used for experimental data, as the virtual counts fluctuate in the same way.

Another minor aspect of the visualization of this graph relates to the fact that the axis scales following the evolution of the variable, in order to always have the best visualization for different power levels.

## 2.5 Operational states



Figure 2.13: Operational states buttons in the simulator.

CROCUS has five operational states, which are also interactive buttons in the control board: "Zero", "Arret", "Attente", "Inter", and "Manuel" [4]. As shown in Figure 2.2, these buttons are also present in the main controls tab of the simulator. Figure 2.13 shows that, to improve the usability of the simulator, the currently selected state is highlighted (as in the real control board), and below the buttons there are thin green and red strips to represent the clickability of the respective button. The latter are especially useful when the "Attente" and "Inter" states are active, because timers were implemented to simulate the real time required to start the reactor. Each state and the links between them are presented in Table 2.3 and thoroughly explained in the following paragraphs.

State	Clickable state buttons	Access to
OFF	ATTENTE	Configurational, operational, and detector parameters
ARRET	OFF <sup>1</sup>	Operational and detector parameters
ATTENTE	ARRET, INTER <sup>2</sup>	Operational and detector parameters
INTER	ARRET, ATTENTE, MANUEL <sup>3</sup>	Operational and detector parameters, neutron source
MANUEL	ARRET, ATTENTE, INTER	Operational and detector parameters, CR and WL <sup>4</sup> , neutron source

Table 2.3: Operational states in the simulator.

Where "Operational parameters" refers to the speeds of the control rods and the spillway, "Detector parameters" refers to the conversion factor and dwell time of the detectors, and "Configurational parameters" refers to the physics settings, the reactivity worths of the control rods and water, and the operational limits (SCRAM signals).

<sup>1</sup>Once the WL has reached 0 mm. If the "Arret" state was activated by pressing the "SCRAM" button, it is necessary to first press the "SCRAM key" button.

<sup>2</sup>After a 9-minute timer.

<sup>3</sup>After an 8-minute timer and if the neutron source is inserted.

<sup>4</sup>Once the WL has reached 800 mm.

### 2.5.1 "Zero" / "Off" state

The state "Zero" in CROCUS corresponds to a particular state in which there is no fuel in the reactor, and maintenance can thus be done. Since this state is not of interest for the simulator, it was replaced with a fictitious state, called "Off". This is the default state the reactor when the simulator is started, and, compared to the real reactor, it represents the state in which the power for the control board is still off. The purpose of this state is to be able to set all the configurational parameters: the physics settings, the reactivity worths of the control rods and water, and the operational limits. This was done to maintain the flexibility of the simulator by allowing the operator to simulate different configurations of CROCUS, while also ensuring a coherent physical behaviour once the reactor is started by preventing the operator from later changing the parameters. In all other operational states, the only parameters which can be modified are the operational and detector ones: the speeds of the control rods and the spillway (as in CROCUS, where they are not fixed), and the conversion factors and dwell time of the detectors. Since the latter ones concern the detectors, they become unmodifiable only during the acquisition (*Start acquisition* button, [subsection 2.2.6](#)).

From the "Off" state, the operator can go only to the "Attente" state.

### 2.5.2 "Arret" state

Once the "Arret" button is pressed, the reactor is shut down: the safety blades are dropped into the reactor, the neutron source is withdrawn from below the core (if it had not yet been), and the valves of the expansion tanks are opened, thus the water level drops to 617 mm. After that, the vessel is automatically emptied at the arbitrary speed of 10 mm/s. The control rods stop and stay at the position they were when the shutdown was activated.

The "Arret" state can be accessed either by pressing the respective button or through a SCRAM or URGENCE shutdown. If the operator presses one of these two buttons, or if an automatic SCRAM is activated, the shutdown happens with the same sequence of events as if they had pressed the "Arret" button, and the reactor is then found in the "Arret" state.

Once the water level has reached 0 mm, the operator can switch from the "Arret" state to the "Off" state, simulating the shutdown of the control board after that of the reactor. If the "Arret" state was accessed by pressing the "SCRAM" button, the "SCRAM key" button must be pressed before being able to press "Off", simulating the need for the SCRAM key after a manual SCRAM.

### 2.5.3 "Attente" state

In the "Attente" state, the operator goes through the checklist and controls the right functioning of the lights while waiting for the water tank to fill up; this takes around 9 minutes. Moreover, some water also enters the vessel, but this was not modelled in the simulator due to a lack of precise values. To simulate the waiting time required for this stage of the start-up, a timer of 9 minutes that prevents the operator from changing states was implemented.

In the "Attente" state, the operator can always press the "Arret" button, and they can also press the "Inter" button if at least 9 minutes have elapsed since the "Attente" state was activated.

#### **2.5.4 "Inter" state**

In the "Inter" state, the water level is automatically increased to 500 mm at the arbitrary speed of 10 mm/s, and the operator waits for the water to reach the desired temperature thanks to the heating system; this takes around 8 minutes. In this state, the operator also controls that the neutron detectors work properly, and to do so it is necessary to insert the neutron source (otherwise, no counts are detected). To simulate this, an 8-minute timer that prevents the operator from changing states was implemented, and the operator is allowed to go to "Manuel" only if the neutron source is inserted.

In the "Inter" state, the operator can always press the "Arret" and "Attente" buttons, and they can also press the "Manuel" if at least 8 minutes have elapsed and the neutron source is inserted.

#### **2.5.5 "Manuel" state**

After pressing the "Manuel" button, the safety blades are automatically withdrawn and the water level rises to 800 mm at the arbitrary speed of 1 mm/s to simulate the wait of 5 minutes before being able to manually operate the reactor. Once the water level has reached 800 mm, the operator can freely move the control rods and maneuver the spillway to raise or lower the water level within the range of the spillway, which is 800 - 1000 mm.

In the "Manuel" state, the operator can press the "Arret", "Attente", and "Inter" buttons. If the "Attente" and "Inter" states were activated from the "Manuel" state, the neutron source is withdrawn, the safety blades are inserted, and the water level is lowered to 500 mm; then there is no need for the timer to go back to "Manuel".

# 3 | Experiments and validation

On 9th May 2025, three experiments were conducted on CROCUS to obtain the reactivity worth curve of the water level and to validate all other aspects of the simulator:

- Reactor period measurements changing the water level.
- Reactor period measurements changing the position of the South control rod.
- Approach to criticality.

Given that the main purpose of the simulator is to be educational for EPFL students, the choice was to validate the simulator with the same experiments that the students conduct on CROCUS during the first semester of the master's program in Nuclear Engineering.

## 3.1 Experimental setup

The experiments were conducted on the CROCUS reactor, described in detail in [section 1.2](#). For all the experiments, the experimental data was retrieved by a fission chamber which contains highly enriched uranium ( $\sim 93\%$ ). The  $^{235}\text{U}$  fissions when hit by thermal neutrons, leading to fission fragments that ionize the gas inside the chamber. This detector works in "pulse mode", meaning that the current generated by the ionized gas collected at the electrodes is integrated over time by a preamplifier to obtain a voltage in the order of mV, which is then amplified to the order of V and "cut" as soon as it starts decreasing (discharge of the RC circuit of the preamplifier). After that, there is a discriminator, which considers as counts only signals coming out of the amplifier above a certain threshold amplitude. This way, no information on energy is retrieved, but only on the number of counts, which is proportional to the number of neutrons. The information on the energy, nevertheless, would be useless since it's the energy of the fission fragments (i.e. the Q-value of the fission) and not that of the neutrons. For safety reasons, the detector check is done at low water levels (in the "Inter" state, see [subsection 2.5.4](#)); therefore, the fission chamber is placed near the bottom of the core, in the reflector region.

The digital system used was the DSA-1000 multi-channel data acquisition system from CAN-BERRA connected to a PC with the GENIE-2000 software installed, which allowed to visualize and record the neutron counts as a function of time. Here is also where the dwell time can be set.

## 3.2 Water level: reactor period measurements

Reactor period measurements were carried out at water levels both above and below criticality, adding positive and negative reactivity insertions to ensure a complete assessment of the reactor response, to be later implemented in the simulator.

### 3.2.1 Experimental method

For each measurement, the reactor was first stabilized by keeping it at the critical water level of 956.2 mm for a few minutes. The dwell time was then set in the data acquisition system, and the measurement was started. After  $\sim 30$  seconds (waiting time), the reactivity was suddenly inserted by regulation of the water level to the desired value.

Each measurement was conducted to roughly capture a change in power, and therefore neutron population, by a factor  $\sim 100$  to have enough data for the fitting. However, this was not always obtained due to time and technical constraints. Once the desired power level was reached, the reactor was returned to a subcritical state in the case of a positive reactivity insertion, and to a supercritical state in the case of a negative one, in order to respectively decrease or increase the power before starting the next acquisition.

**Table 3.1** presents the water levels to be reached decided for the period measurements, the starting and final power values, and the dwell times used in the measurements.

Water level [mm]	Starting power [W]	Ending power [W]	Dwell time [s]
$925 \pm 0.1$	10.7	0.2	0.080
$935 \pm 0.1$	9	0.15	0.080
$965 \pm 0.1$	1.3	11	0.200
$975 \pm 0.1$	0.2	13	0.080
$985 \pm 0.1$	0.2	20	0.040

Table 3.1: Water levels and measurements' details.

### 3.2.2 Data analysis

For each water level period experimental measurement, a reactivity value was calculated based on the reactor period, the latter obtained through a fitting of the detector data.

Assuming point kinetics, the first step involved solving the in-hour equation ([Equation 28](#)) to find the seven roots ( $\omega_i$ ) characterizing the evolution of the neutron population (or power), described by [Equation 29](#). The in-hour equation is the solution of the PKE ([Equation 1](#) and [Equation 2](#)) in the case of a step change in reactivity.

$$\rho = \Lambda\omega + \sum_{i=1}^6 \frac{\beta_i\omega}{\lambda_i + \omega} \quad (28)$$

$$\frac{P(t)}{P(0)} = \sum_{i=1}^7 B_i e^{\omega_i t} \quad (29)$$

In order to do so, a first guess value of reactivity needed to be provided. The reactivity value prompted as a first guess for the solution of [Equation 28](#), presented later in [Table 3.2](#), was obtained by running the same experimental setup inside the to-be-updated version of the CROCUS simulator. A preliminary assessment of the simulator's accuracy was carried out, as further explained in [subsection 3.2.3](#), concluding that there was good agreement. Although this simulator-derived value did not yet reflect an accurate calibration of reactivity worths, it was considered a suitable first guess to initialize the calculation. The computed roots were then used to calculate the coefficients  $B_i$  defined by [Equation 30](#).

$$B_i = \frac{\Lambda + \sum_{j=1}^6 \frac{\beta_j}{\omega_i + \lambda_j}}{\Lambda + \sum_{j=1}^6 \frac{\beta_j \lambda_j}{(\omega_i + \lambda_j)^2}} \quad (30)$$

Since the asymptotic exponential behaviour of the neutron population emerges only after the decay of the higher modes, an adjustment time had to be removed from the fitting so that this initial transient region did not influence the result. This was done by evaluating the relative contribution of the dominant (fundamental) mode compared to the total kinetic response, where also the 6 other roots are taken into account. The adjustment time was defined in [Equation 31](#) as the point beyond which this relative difference falls below a set threshold, indicating that the transient is sufficiently governed by the slowest exponential mode to allow reliable period estimation. The threshold used was 1% for all reactivity insertions except the one to 925 mm, set to 5% to have enough statistics for the fitting. The adjustment times calculated through this definition are presented in the results chapter, in [Table 3.2](#).

$$\left| \frac{B_1 \exp(\omega_1 t) - \sum_{i=1}^7 B_i \exp(\omega_i t)}{\sum_{i=1}^7 B_i \exp(\omega_i t)} \right| < 0.01 \quad (31)$$

The neutron count signal of each experiment was then analyzed starting from this computed adjustment time, which was added to the waiting time before the reactivity insertion, which was confirmed visually. For positive reactivity insertions, the fitting time interval was truncated slightly before the peak of the detected data to prevent any influence from statistical fluctuations around the peak in the transition to the subcritical state. The selected portion of the experimental data was then fit to an exponential function of the form:

$$P(t) = B_1 e^{\omega_1 t} \quad (32)$$

with  $\omega_1$  being the fundamental root of the in-hour equation, corresponding to the inverse of the reactor stable period  $\tau$ .

To account for the statistical nature of the measured counts  $N$ , uncertainties were modelled according to Poisson statistics, with the standard deviation at each point equal to  $\sqrt{N}$ . A Monte Carlo procedure was then used to estimate the uncertainty of the fitted  $\omega$ : 10000 samples were generated by drawing Poisson-distributed values around the measured counts, and the exponential model was fit separately to each sample using non-linear least squares optimization.

The resulting distribution of fitted  $\omega$ 's was then used to compute the mean value and standard deviation as estimates of the best-fit  $\omega$  and its associated uncertainty.

The corresponding distribution of reactivities associated with each water level was obtained by applying the in-hour equation to the sampled omega values, directly propagating their uncertainties. The mean and standard deviation of this reactivity distribution were then reported for each water level.

These last experimentally derived reactivities were then plotted against the water level to obtain the simulator's water level reactivity curve described in [subsection 2.3.1](#) to finalize the reactivity worth of water in the simulator.

The experiment was then carried out in the simulator following the same procedure, and its output is compared to the experimental measurements in the validation section ([subsection 3.2.5](#)).

### 3.2.3 Validation with prior experiments

Initially, the reactivity worth curve for the water level was obtained, with the same methodology explained in [subsection 2.3.1](#), using the results of the experiments conducted during the winter semester on reactor period measurements [2]. The simulator was then used to reproduce the same steps in order to assess its accuracy prior to the refinements needed for the final validation.

The data obtained from the detectors was compared to the same experiment run on the simulator, setting the corresponding dwell time, and is presented in [Figure 3.1](#) for the period measurement of the water level at 985 mm. A similar trend was found in the other measurements.

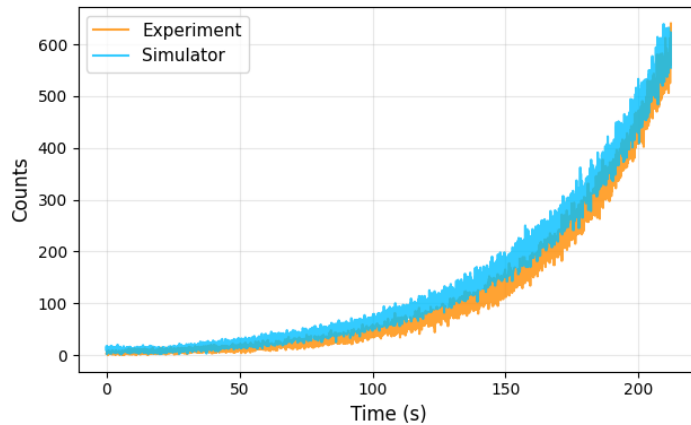


**Figure 3.1:** Comparison of reactor period measurements at  $WL = (985 \pm 0.1)\text{mm}$  between the to-be-updated simulator and the experimental data.

It can be noted how the real measurement shows a slightly sharper exponential increase, besides the overestimation of the number of counts of the simulator from the beginning; this is due to the different reactivity corresponding to the water levels. As can be grasped from the picture, the reactor period is larger for the simulator, so the power growth is slower; it follows

that reactivity is lower for the simulator. This finding suggests that the reactivity curve for the water level is different and/or the critical water level at the time of the experiment was not the one set in the simulator.

This preliminary assessment showed that some improvements and adaptations should follow, but the simulator was already capable of producing acceptable results that could be used as a first guess for the reactivity calculations described in [subsection 3.2.2](#).

### 3.2.4 Results

Following the methodology described in the [subsection 3.2.2](#), the adjustment times removed from the fitting for each water level experiment are presented in [Table 3.2](#), together with the first guess value of reactivity used, coming from the previous version of the simulator.

Water level [mm]	First guess $\rho$ [pcm]	Adjustment time [s]
$925 \pm 0.1$	-140.8	248.16
$935 \pm 0.1$	-93.8	321.68
$965 \pm 0.1$	34.6	42.02
$975 \pm 0.1$	73.5	46.48
$985 \pm 0.1$	110.7	41.81

Table 3.2: First guess reactivity and adjustment time for different water levels.

The numerous exponential fittings from the Monte Carlo procedure were generated, and the mean value of the reactor period was found for each water level change. An example of this is shown in [Figure 3.2](#) for the case of the data retrieved from a water level increase to 975 mm.

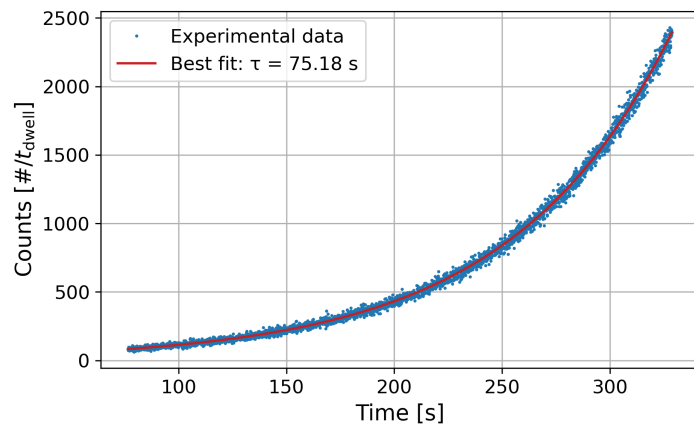


Figure 3.2: Exponential fitting to find the reactor period - 975 mm case.

Finally, the values of reactivity calculated for each water level variation, together with their uncertainties, are presented in [Table 3.3](#). These were necessary to build, through a fitting, the water curve described in [subsection 2.3.1](#), which, once implemented in the simulator, generated the values shown on the right in the same table.

It can be noticed that the uncertainties on  $\rho$  obtained for the subcritical water levels are significantly larger. This is not due to the noise on the counts because the measurements were

conducted approximately across the same power interval (0.1 W to 10 W). Instead, it is mainly due to the fact that, in those cases,  $\omega$  was obtained from a fit over fewer points. This is because the higher modes decay much more slowly relative to the fundamental one compared to the cases where the main exponent is positive. This is because for negative reactivity insertions also the fundamental mode is a negative exponential.

Water level [mm]	Experimental $\rho$ [pcm]	Simulated final $\rho$ [pcm]
925 ± 0.1	-171 ± 8	-161.6
935 ± 0.1	-106.6 ± 1.8	-106.6
965 ± 0.1	38.62 ± 0.04	40.3
975 ± 0.1	82.46 ± 0.07	83.3
985 ± 0.1	123.28 ± 0.09	123.3

Table 3.3: Reactivity results of the reactor period measurements conducted by changing the water level with both control rods fully extracted.

### 3.2.5 Validation of the simulator

In order to assess the accuracy of the simulator in representing the actual reactor behaviour, the same experiments carried out on CROCUS were replicated on its simulator, following the methodology described in [subsection 3.2.1](#). The counts measurement was obtained in the same manner, taking into account the waiting time before the reactivity insertion and setting the same dwell time on both the CROCUS data acquisition system and the simulator.

It is important to note that the power value noted during the real experiment ([Table 3.1](#)), used later in the simulator as the initial condition for each reactivity insertion, was subject to rapid temporal fluctuations. The reading was purely instantaneous, not stored, and therefore inaccessible for subsequent averaging. In addition, its precision was limited due to low significant digits, resulting in considerable uncertainty. Therefore, the logged value should be interpreted with caution, as it may not accurately reflect the actual reactor power at any given moment. For this reason, some simulations were slightly adjusted, within the uncertainty bounds, to better match the count rate corresponding to the initial power level at the start of the measurement.

For each water level acquisition, a normalized residual metric was adopted to show the agreement between the two data sets. For each time step, i.e. integration time, the residuals  $R(t)$  were calculated as:

$$R(t) = \frac{C_{CROCUS}(t) - C_{Simulator}(t)}{C_{CROCUS}(t)} \quad (33)$$

Where  $C_{CROCUS}(t)$  and  $C_{Simulator}(t)$  denote the neutron count rates measured experimentally and predicted by the simulator, respectively. This metric quantifies the relative deviation of the simulation from reality, making the comparison independent of absolute scaling and thus more sensitive to discrepancies in the reactor response behaviour.

Given that the experimental measurements are affected by statistical fluctuations intrinsic to neutron counting, and the same behaviour was reproduced in the simulator as previously dis-

cussed in subsection 2.4.2, the uncertainty associated with the residuals was estimated via a Monte Carlo approach. For each measurement, 10000 independent simulations of both the experimental and simulated counts were sampled by assuming normally-distributed random fluctuations with a standard deviation equal to the square root of the counts.

From the collection of all Monte Carlo runs, the standard deviation of the residuals was computed at each time point, and confidence intervals corresponding to the  $1\sigma$  (i.e., the 15.85<sup>th</sup> and 84.15<sup>th</sup> percentiles) were extracted.

A challenging aspect concerned the speed of the movable spillway system that determines the water level. In the CROCUS control board, this speed is manually regulated by the operator through a joystick, with no real-time indication of its value. Since this parameter must be explicitly defined in the simulator, an initial set of simulations was performed using the default value of 2.2 mm/s, as reported in the safety report [4]. However, a preliminary comparison with experimental data revealed a noticeable shift in the response curves, suggesting a delay in the water level's effect on reactivity for the real reactor case. This was further confirmed by a constant offset along the time axis in the residual plots, especially visible in the 975 mm case. This is presented in figure Figure 3.3b, together with the output data from the real and simulated measurements plotted on the same graph Figure 3.3a. The residuals plots for the other measurements are presented in Figure 3.5. Please note that the insertion starts 30 seconds after the measurement has begun, hence the close match at the beginning of each plot.

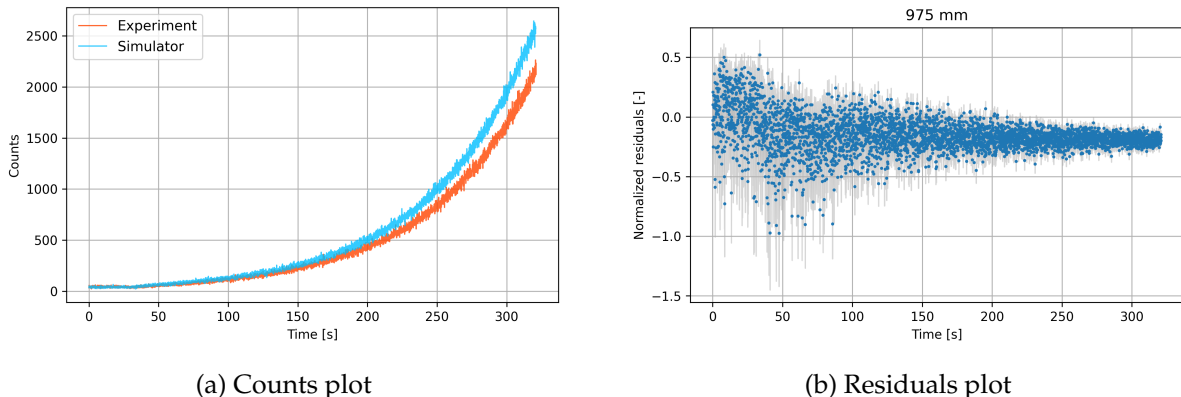


Figure 3.3: Results of the measurement at  $WL = 975$  mm, with spillway speed of 2.2 mm/s.

To address this, an alternative set of simulations was conducted, reducing the spillway speed to 0.5 mm/s, chosen arbitrarily based on the noted start and end times of the water level change. This second run produced a visibly better agreement with the experimental results, as can be observed in detail in Figure 3.4 for the 975 mm case.

The residual plots of the complete set of measurements with this adapted velocity are presented in Figure 3.6. In the graphs, the residuals calculated at each time step  $R(t)$  are plotted with blue dots. The grey envelope represents the  $1\sigma$  confidence interval.

These plots presented in Figure 3.5 and Figure 3.6 illustrate not only the average deviation of the simulated value from the experimental one, but also the expected variability due to

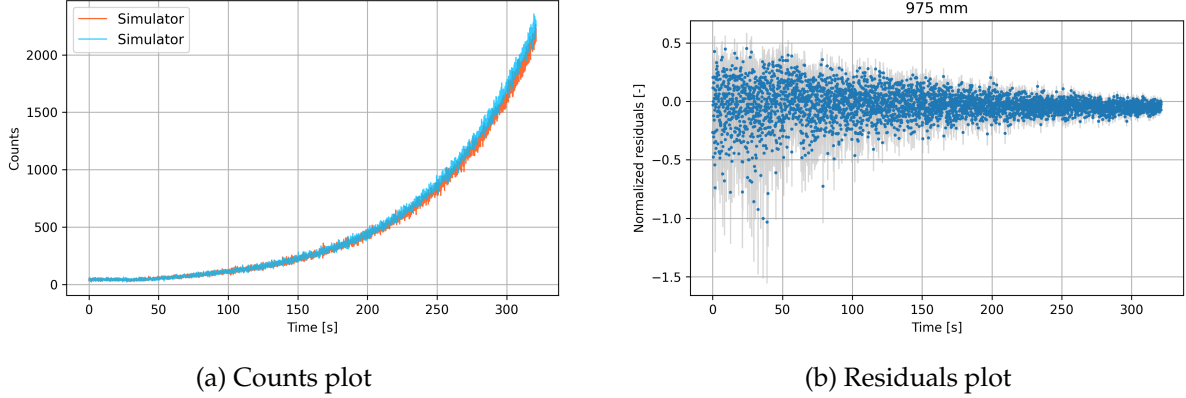


Figure 3.4: Results of the measurement at  $WL = 975$  mm, with spillway speed of  $0.5$  mm/s.

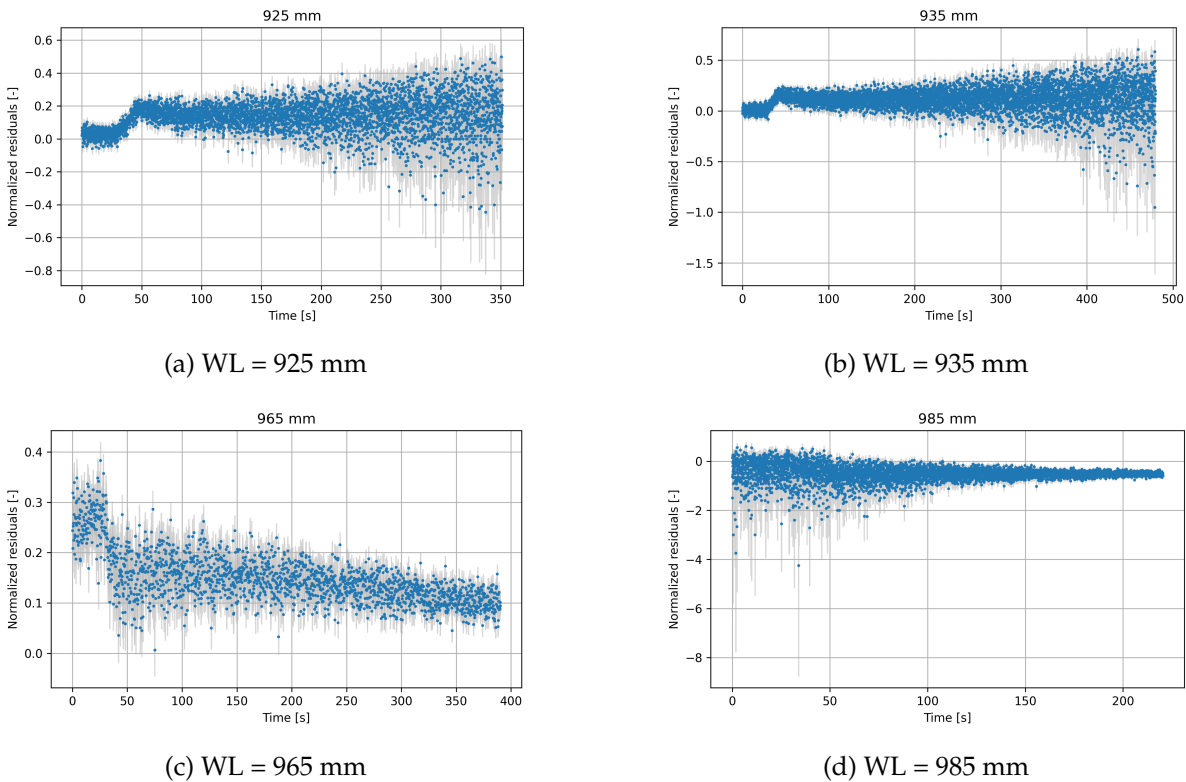


Figure 3.5: Residuals plots for measurements at different water levels, spillway speed set at  $2.2$  mm/s.

statistical noise. It can be observed that the uncertainty on the residuals is larger where the neutron counts are less (i.e. at low power, corresponding to the initial region for a positive insertion of reactivity and the ending region for a negative one). This is due to the Poissonian distribution, for which the relative uncertainty  $\sqrt{N}/N$  is larger for small values of  $N$ .

Considering the region with smaller uncertainties, for positive reactivity insertion, the round of simulations carried out with a lower spillway speed resulted in residuals below  $0.2$  for the  $965$  and  $975$  mm cases, and still below  $0.5$  for the  $985$  mm one, showing conformity with the expected physical behaviour.

For the negative reactivity insertion experiments, a worsening of the results was observed in-

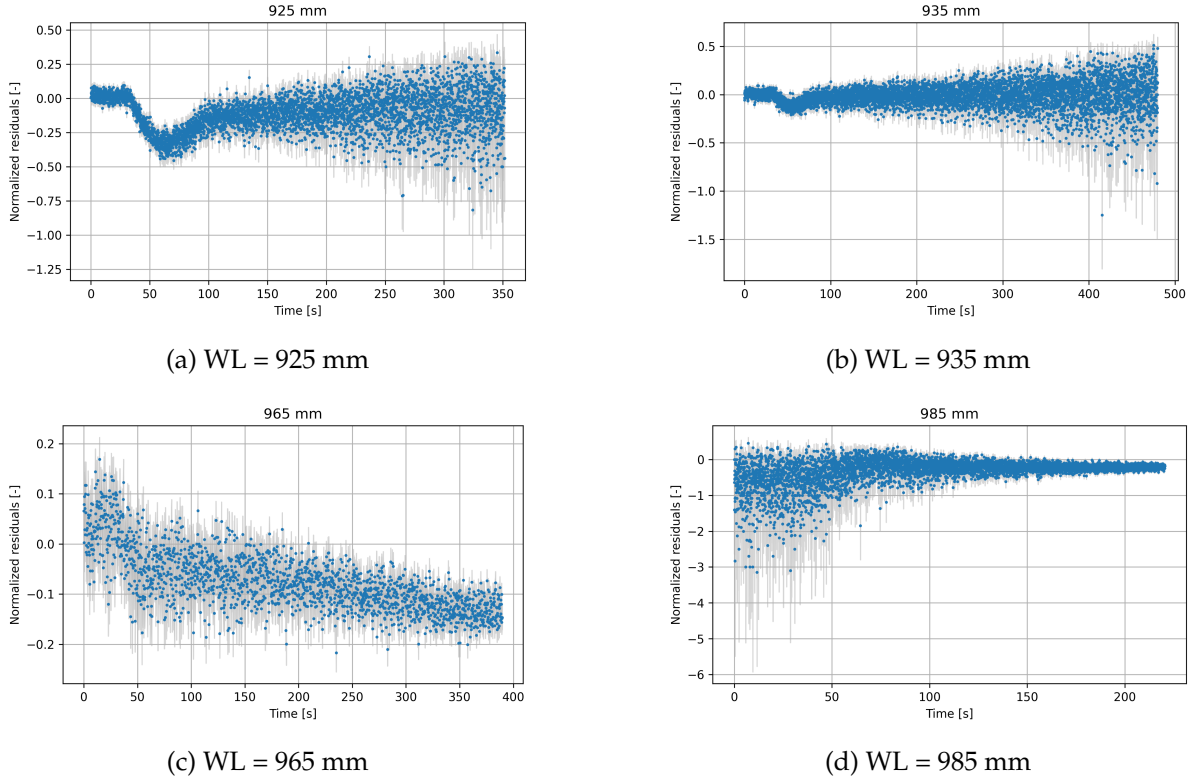


Figure 3.6: Residuals plots for measurements at different water levels, spillway speed set at 0.5 mm/s.

stead. It is believed that the reason for this behaviour is attributable to the irregularity of the spillway speed when maneuvered via the control board. When using the manual joystick to adjust the water level to the desired position, the reactor operator uses a higher speed at the beginning, and slows down when closer to the end point for fine positioning. In most experiments, this lack of precision is not relevant; however, when the measurements are compared to a simulation carried out with constant spillway speed, this difference plays a role. The discrepancy is bigger in the slower simulation, where the sharp decrease observed in the residuals (see [Figure 3.6a](#)) once the reactivity is inserted ( $\sim 30$  s) reflects the much higher velocity of the joystick.

Lastly, from all the plots, especially the ones representing the faster spillway case, the reactivity prompt jump can be glimpsed at around 30 s. The simulator is able to reproduce it effectively, whereas it is not clearly visible from the CROCUS measurements.

### 3.3 Control rods: reactor period measurements

Following the reactor period measurements performed via water level variation, an additional series of experiments was carried out to validate the control rod worth curves by estimating the reactivity associated with sudden control rod (CR) withdrawals.

### 3.3.1 Experimental method

Control rod speed for CROCUS was such that a total withdrawal could be made in 5s. With a water level of 990 mm, the reactor is critical with one rod inserted at 260 mm.

For all measurements, the reactor was initially stabilized at the water level of 990 mm with the North CR completely extracted and the South CR partially inserted. This last one was then extracted according to predefined stroke lengths, reaching a final position of 500, 750 and 1000 mm, the latter corresponding to a full extraction. As in the water level case, a time of  $\sim 30$  seconds was waited from the start of the acquisition before the extraction, and the dwell time was set beforehand in the data acquisition system. As in the previous experiment with the water level, each measurement aimed at observing a significant power change (factor  $\sim 100$ ) to ensure sufficient statistics for the reactivity estimation via fitting.

The details specific to the measurements are presented in [Table 3.4](#), including the reactor power recorded at the beginning and end of each extraction. It can be noticed that the initial CR position is slightly different between the measurements: this is due to the fact that the reactivity worth difference between these positions is minimal, and it was therefore difficult to assess whether the reactor was in a critical state or not.

CR position [mm]	Starting power [W]	Ending power [W]	Dwell time [s]
260 → 500	0.3	11	0.200
270 → 750	0.1	13	0.040
275 → 1000	0.6	21	0.040

Table 3.4: Control rod extraction configurations used for reactor period measurements.

### 3.3.2 Data analysis

The same data processing methodology used in the water level variation experiments was applied to the control rod extraction cases. Following the experiment description, the simulator was used out to find the reactivity to input as a first guess for the calculation of the seven  $\omega$  roots of the inhour equation ([Equation 28](#)). The adjustment time was obtained by means of [Equation 31](#) using a threshold of 1%. Reactor periods were then obtained by fitting the count rate, and reactivity values were then derived from these periods using the inhour equation.

### 3.3.3 Results and validation

The reactivity values given as first guess inputs, together with the calculated adjustment times, are presented in [Table 3.5](#) for the three measurements.

CR final position [mm]	First guess $\rho$ [pcm]	Adjustment time [s]
500 $\pm$ 0.1	58.8	47.2
750 $\pm$ 0.1	123.6	39.4
1000 $\pm$ 0.1	142.1	36.6

Table 3.5: First guess reactivity and adjustment time for different rod extraction positions.

The values of the calculated reactivity from the experimental results, and the reactivity values generated by the simulator (equal to the first guess values), are reported in [Table 3.6](#). It is worth mentioning that at the initial conditions set during the real experiment (water level position at 990 mm, and one control rod fully extracted), the critical state of the reactor was assessed to be reached with the other control rod at 260 mm. The same conditions in the simulator yield a reactivity worth of -3.3 pcm, a slightly subcritical state.

CR final position [mm]	Experimental $\rho$ [pcm]	Simulated $\rho$ [pcm]
500 $\pm$ 0.1	63.70 $\pm$ 0.05	58.8
750 $\pm$ 0.1	127.35 $\pm$ 0.12	123.6
1000 $\pm$ 0.1	143.05 $\pm$ 0.17	142.1

[Table 3.6](#): Reactivity results of the reactor period measurements conducted by changing the position of the South control rod with a water level of (990  $\pm$  0.1) mm.

The CR extraction experiments were simulated in the CROCUS simulator following the same protocol as in [subsection 3.2.5](#). The same dwell times and power conditions were applied in the simulations. An issue identified in this step was the lack of precise knowledge about the actual speed of the control rod during extraction. Therefore, simulations were first carried out assuming a CR speed of 0.5 m/s. However, these results showed poorer agreement with experimental data, as revealed by the residual plots presented in [Figure 3.7](#).

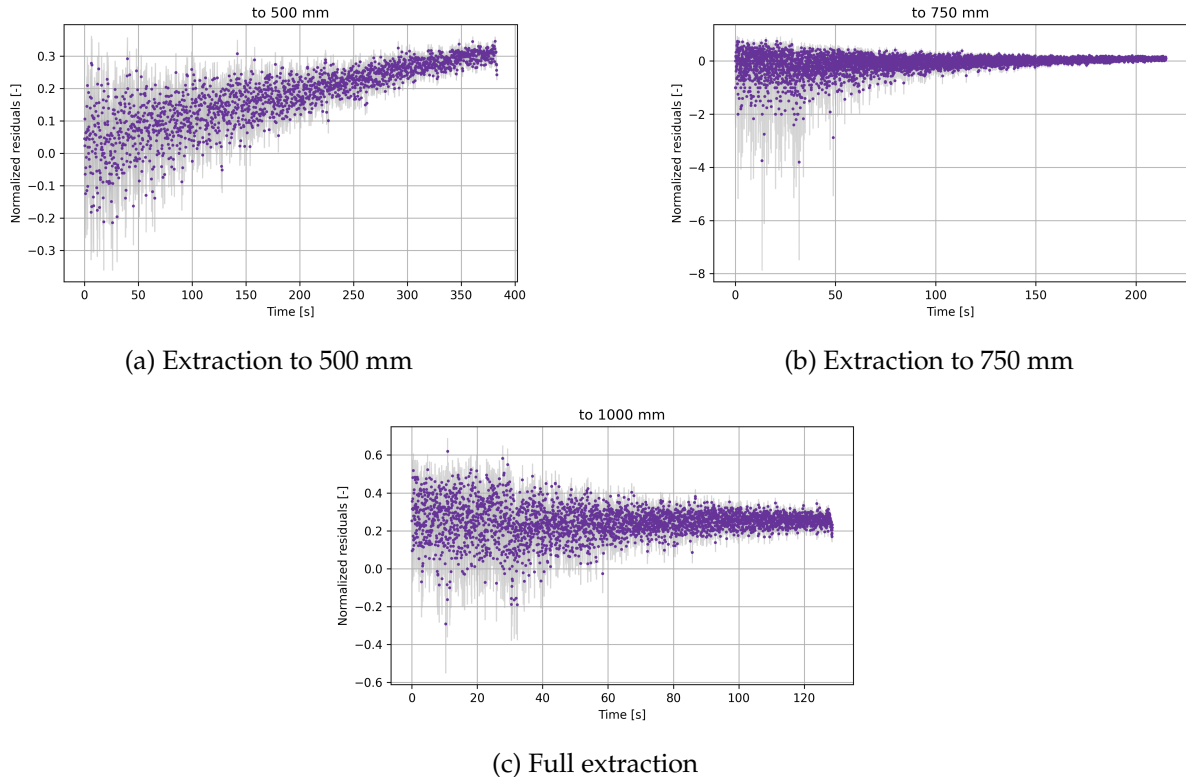


[Figure 3.7](#): Residual plots for different control rod extractions - 0.5 m/s speed.

A second set of simulations was performed using a speed of 1 m/s to mimic a full extraction in 1 s. This simulation led to a notably better match with the experimental data across all three

CR extraction cases, as can be seen from [Figure 3.8](#).

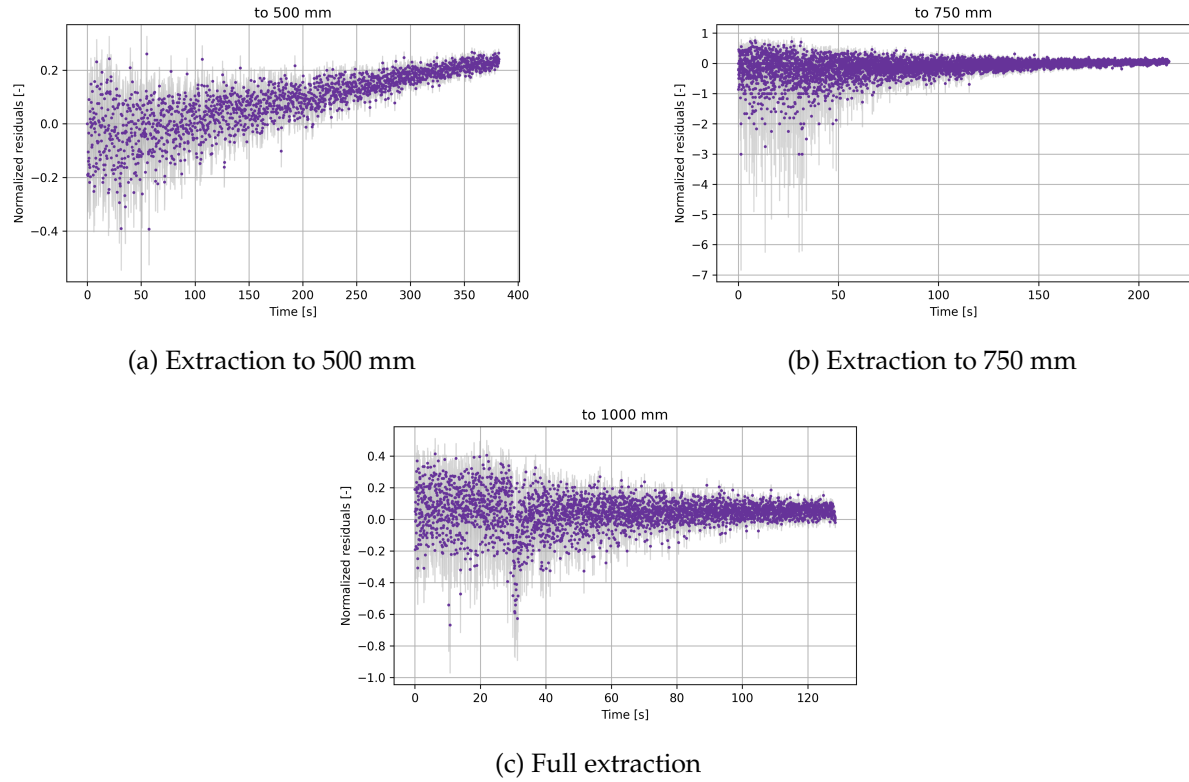


Figure 3.8: Residual plots for different control rod extractions - 1 m/s speed.

Similar considerations to the water level variation experiment can be drawn. At higher counts, towards the end of the residuals plots, better statistics can be observed due to the reduction of the Poissonian influence. Here, residuals lower than 0.2 can be observed for the higher speed case, suggesting good agreement between the real and simulated measurements.

The case of CR withdrawal to 500 mm shows, however, an increasing trend in the residual plot. It is believed that these results can be explained based on the assumption made for the control rod curves (described in [subsection 2.3.2](#)). Since in the experiment the water level is instead set at 990 mm, the worth associated with each coordinate is indeed slightly shifted. The differential rod worth is much higher at mid-height (see [Figure 2.4](#)); therefore, when the extraction is made up to this point, the integral worth is lower in the simulated case compared to the real one. Going up in height in the S-curve, the slope becomes much less pronounced, and, consequently, the total rod worth up to that point diverges much less. This explains why, with the same inaccurate assumption, the trend is no longer visible for the extractions to 750 and 1000 mm.

Considering that, because of the limited excess reactivity of the reactor ([Table 2.2](#)), the experiments with the control rods can be conducted with a water level set in a restricted range (at water levels much lower than 1000 mm, criticality cannot be reached with one control rod inserted), it is possible to state that the assumption of no dependency between the CR and WL curves is valid. The discrepancies between the simulated and real results can be attributed to this assumption (the implemented CR curve was obtained with a WL of 1000 mm); how-

ever, they are negligible given the goal of the simulator, which is to be educational rather than strictly accurate.

## 3.4 Approach to criticality

### 3.4.1 Experimental method

The approach to criticality experiment that was conducted was a simulation of what students would do during such an experiment. Since the focus was more on validating the simulator than on finding the critical water level of the reactor, the experiment was not conducted as one normally would, also because the critical water level was already known to be  $(956.2 \pm 0.1)\text{mm}$ .

Neutron detection counts were obtained with the fission chamber described in [section 3.1](#) at the water levels and for the time intervals reported in [Table 3.7](#). The dwell time was set at 1 s.

Water level [mm]	Time [m:s]
$800.9 \pm 0.1$	10:42
$900 \pm 0.1$	10:30
$920 \pm 0.1$	10:24
$940 \pm 0.1$	9:34
$950 \pm 0.1$	11:11

Table 3.7: Experimental method of the "Approach to criticality" experiment.

After taking these measurements, the water level was raised to  $(956.1 \pm 0.1)\text{mm}$ , and after 1 minute and 42 seconds, the neutron source was removed.

Unlike in a normal approach to criticality, the chosen water levels did not follow a strictly well-reasoned choice based on the value of the extrapolated critical water level; instead, they were chosen based on the prior knowledge of the real critical water level.

### 3.4.2 Data analysis

No data analysis was performed on the results of the experiment, meaning that no extrapolation was done to estimate the critical water level. The reasons for this choice are two: the first is that this was not the goal of the experiment, which was conducted purely to validate the simulator, the second is that, as later shown in [Figure 3.9](#), the time interval chosen for the measurement at  $(950 \pm 0.1)\text{mm}$  was not long enough to let the system reach a stable state; therefore, the results would not be accurate nor precise.

### 3.4.3 Validation of the simulator

The same experiment was conducted on the simulator, and [Figure 3.9](#) shows the comparison between the cumulative acquired data of the real experiment and the simulated experiment. To compare the two results more quantitatively, normalized residuals were calculated as shown in [Equation 33](#), and a Monte Carlo method was applied as explained in [subsection 3.2.5](#). The resulting plot is shown in [Figure 3.10](#); the grey envelope shows the  $1\sigma$  confidence interval.

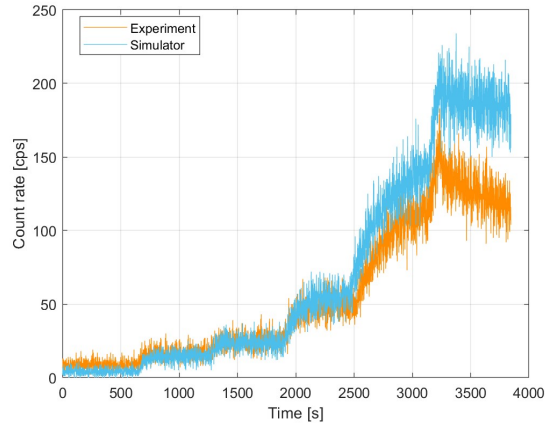


Figure 3.9: Counts recorded by the fission chamber each second from subcriticality to criticality.

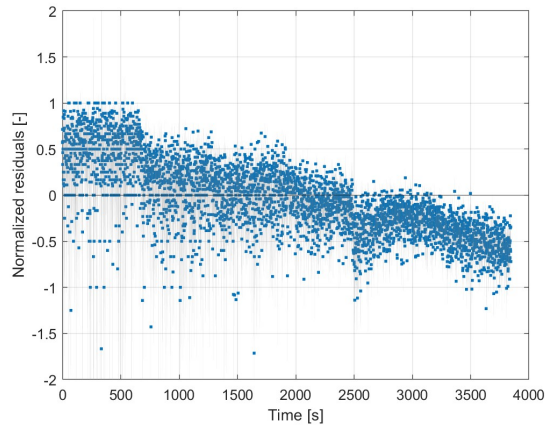


Figure 3.10: Residuals plot for the approach to criticality.

These results show an offset between the experimental and simulated data. The discouraging aspect is that the offset changes sign between the lowest and highest water levels, which cannot be explained by a mistake in the conversion factor of the simulated detector or the intensity of the neutron source. The encouraging aspect is that the overall trends of the curves are the same; it is especially noteworthy the fact that also in the simulator the count rate at  $(950 \pm 0.1)\text{mm}$  does not stabilize over the given time interval.

# 4 | Discussion and conclusion

## 4.1 Discussion

### 4.1.1 Accuracy and performance

While not primarily developed for high-accuracy simulations, the simulator demonstrates a satisfactory level of agreement, as shown in the experimental validations ([chapter 3](#)). Complete accuracy was never a priority for the development of the simulator, considering that the main goal was to build an educationally valid tool for students. Furthermore, the variety of experimental campaigns continuously performed on CROCUS is a source of unpredictable changes in configurations; this means that even an accurate simulator would very likely become inaccurate in the near future. Having that in mind, the accuracy achieved and confirmed by the experimental results is appreciable enough to state that the simulator qualitatively behaves as CROCUS, as the trends match despite the offsets. Quantitatively speaking, performing experiments on the simulator rather than on CROCUS may, in some cases, lead to different results, which are anyway similar enough to convey the same information and learning insights. In better cases, the quantitative results also fall within the  $1\sigma$  confidence interval of the experimental data, meaning that the simulator fully succeeds at emulating CROCUS behaviour.

From an operational point of view, the performance of the simulator is much better. The idea behind the development of the GUI was to best represent the CROCUS control board, in order to allow the user to engage with the simulator from a perspective closely resembling a real operator's role. The presence of the operational states, the reactor startup steps, and the real-time displayed graphs, allows the simulator to facilitate users in familiarizing themselves with the real CROCUS control interface.

### 4.1.2 Educational value

The main strength of the simulator is its educational value. The context of the project at hand is that the students of the master's program in Nuclear Engineering at EPFL-ETH are not allowed, for regulatory and safety reasons, to operate the real reactor. This partially limits the learning potential of the experiments they conduct on the reactor because they miss the opportunity to learn how a research nuclear reactor is operated, focusing mainly on the physics behind it. With this tool, students are encouraged and given the possibility to familiarize themselves with the control board and some of the various operational settings, which can then also

result in a more active engagement in the control room during the experiment. Furthermore, the simulator allows the students to eventually repeat part of an experiment if something was not clear during the limited time they spent in the control room.

Several important aspects of experimental reactor physics can be better understood simply thanks to a longer exposure to them in the simulator. To list a few examples, the Poissonian distribution of the count rate, the dwell time, and the reactivity curves are well presented in the simulator and, at the same time, typically not the clearest concepts for students.

Finally, having a simulator which is also reasonably accurate ensures that simulations yield plausible results that faithfully resemble the behaviour of CROCUS. This allows the students to explore new operational conditions and the corresponding reactor responses. This is especially beneficial when the control rods are not available for student experiments, which was the case, for instance, in the winter semester of 2024.

#### 4.1.3 Limitations

The limitations of the simulator stem from the assumptions and simplifications made (see [section 2.1](#)). Regarding the reactivity feedback effects, recent experimental results confirm that the operational temperature has a non-negligible influence on the reactivity.

The main limitation, which is also the main reason for the discrepancy between the experimental results and the simulator results (see [chapter 3](#)), is the speed of the water spillway, further discussed in [subsection 3.2.5](#). In reality, the operator adjusts the water level by moving a control lever, and the degree to which the lever is tilted determines the speed of the spillway. For this reason, the water level speed is never constant, contrary to how it was implemented in the simulator. A similar problem applies to the movement of the control rods, where the actual functioning should be better understood and implemented accordingly.

From a simulation point of view, assuming point kinetics is valid but still neglects the spatial effects, which are of interest especially for the insertions of the control rods. Furthermore, the complexity of the count rate fluctuations was not fully described, meaning that no neutron noise can be detected because the count rate was implemented such that it follows a Poissonian distribution.

#### 4.1.4 Potential improvements

Some of the potential improvements that could be added to the simulator reduce its limitations. Adding a non-Poissonian distribution of the detected counts, possibly using the results of a neutron noise experiment, would allow students to replicate that experiment on the simulator as well. Implementing inertia and fluid dynamics, especially for the water spillway, would strongly reduce the limitation that the constant speed imposes.

Other potential improvements include the implementation of a dependency between the reactivity curves of the control rods and the water level, instead of just using the curve obtained for a water level of 1000 mm.

Additionally, some graphical improvements could easily be implemented to enhance the user

experience. For instance, in the "Control rods" tab, presented in [Figure 2.3](#), the reactivity curve and its derivative for the water level should be presented only over the range 800 - 1000 mm. This is because in the range from 0 to 800 mm, the curves were obtained assuming a linear trend without any theoretical basis, as no studies on it were found in the literature. That range should hence not be displayed as if it were obtained from real data.

Finally, a future plan could be to connect the simulator to a physical console to also physically simulate the control board. This console should have a joystick lever to move the water level, SCRAM and URGENCE buttons, buttons for the operational states and the neutron source, a light to show the position of the safety blades, and two screens to display the doubling time and the count rate.

## 4.2 Conclusion

In conclusion, while the simulator was not developed with research-grade accuracy in mind, it fulfills its primary purpose of being an effective educational tool. The level of accuracy achieved is sufficient to represent the qualitative behaviour of CROCUS, and in optimal cases, the results also align quantitatively within a  $1\sigma$  confidence interval. This makes the simulator a reliable platform for learning, even if not suitable for detailed experimental analysis.

Its greatest value lies in its ability to bridge the gap between theory and practice. Given that students are not permitted to operate the actual reactor, the simulator offers a meaningful alternative, allowing them to explore reactor operations, interact with control elements, and eventually revisit experimental scenarios.

Although some limitations remain, they are mostly due to necessary simplifications and assumptions. Importantly, these constraints also highlight clear opportunities for future development, whether through improved physical modelling, enhanced user interfaces, or potential integration with physical hardware.

Ultimately, the simulator offers a well-balanced combination of usability, realism, and educational value. It supports a deeper understanding of reactor physics and operations and stands as a strong complement to the hands-on learning experience provided at CROCUS.

## 5 | Authors' contributions

For the initial steps, Caterina Frau removed the superfluous components from the JSI base code, while Matteo Meneghini retrieved CROCUS data. Together, they discussed and selected the appropriate assumptions and simplifications.

A significant portion of the work was dedicated to ensuring that each implementation was properly reflected in the GUI; the corresponding part in the code was modified by the person responsible for each implementation. Matteo implemented the modifications to the definition of the reactivity, taking care of the water level and control rods. Caterina modified the displayed graphs and worked on the corresponding quantities, aiming for a more realistic representation of the CROCUS control board. Matteo implemented the operational states and modified the SCRAM activation and sequence of events. Finally, Caterina implemented the simulated detectors and the possibility to save the simulation data.

The experiments were conducted with the help and under the supervision of Dr. Vincent Lamirand and Cecilia Montecchio, who operated the reactor and the acquisition setup, respectively. Caterina and Matteo chose and defined which experiments were best suited for the validation of the simulator. Afterwards, they both performed the data analyses to double-check the results. Lastly, the simulated experiments for the validation were split between the two students and the results were analysed together.

# Bibliography

- [1] P. Frajtag et al. "Description of the CROCUS reactor". In: *Reactor experiments and radiation detection*. EPFL, 2024, pp. 153–155.
- [2] F.L. Heiniger et al. *Reactor Period Measurements: Radiation and Reactor Experiments*. École Polytechnique Fédérale de Lausanne, 2024.
- [3] International Atomic Energy Agency. *Protocol: Control Rod Calibration*. IAEA Nucleus repository. Protocol prepared in Switzerland. 2018. URL: <https://nucleus.iaea.org/sites/connect/RRIHpublic/CompendiumDB/Shared%20Documents/Switzerland/Protocols%20in%20PDF/Protocol%20Control%20Rod%20Calibration.pdf>.
- [4] V. Lamirand. *Installation nucléaire CROCUS: Rapport de sécurité*. Internal Report 17-48. LRS, 2017.
- [5] J. Malec, D. Toškan, and L. Snoj. "PC-based JSI research reactor simulator". In: *Annals of Nuclear Energy* 146 (2020), p. 107630. DOI: [10.1016/j.anucene.2020.107630](https://doi.org/10.1016/j.anucene.2020.107630). URL: <https://doi.org/10.1016/j.anucene.2020.107630>.
- [6] J.M. Paratte et al. "A benchmark on the calculation of kinetic parameters based on reactivity effect experiments in the Crocus reactor". In: *Annals of Nuclear Energy* 33.8 (2006), pp. 739–748. DOI: [10.1016/j.anucene.2005.09.012](https://doi.org/10.1016/j.anucene.2005.09.012). URL: <https://doi.org/10.1016/j.anucene.2005.09.012>.

# A1 | Appendix

## A1.1 Additional material

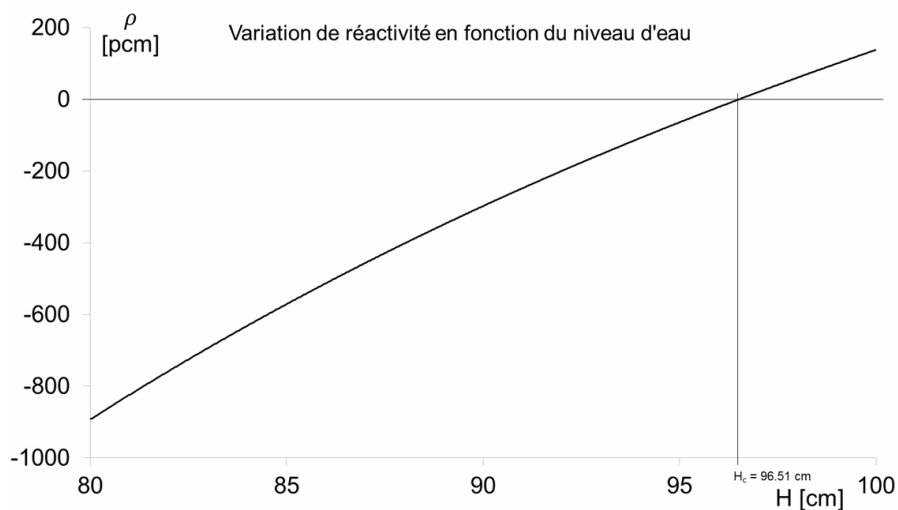


Figure A1.1: Reactivity worth of the water documented in the safety report [4].

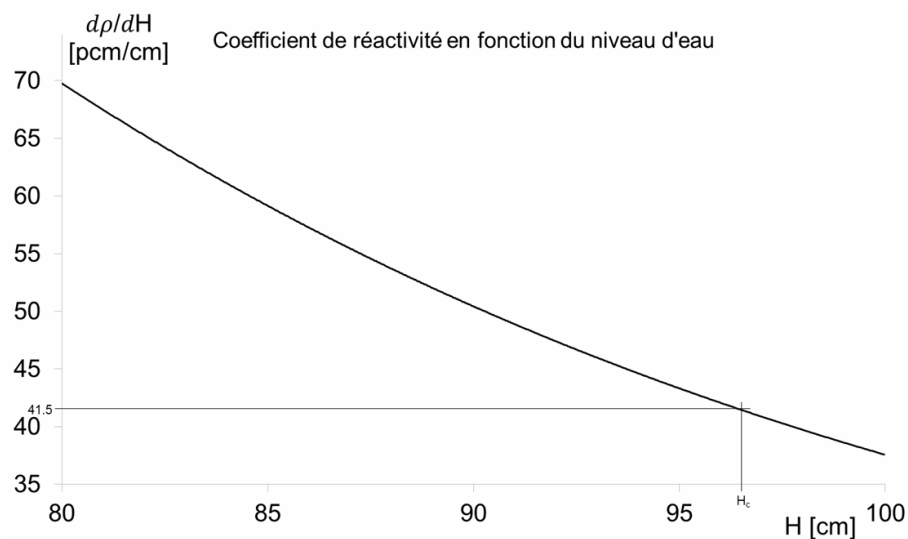


Figure A1.2: Derivative curve of the reactivity worth of the water documented in the safety report [4].